

Structure-Function Studies of Iron-Sulfur Enzyme Systems

Rosmarie Friemann

*Department of Molecular Biology
Uppsala*

**Doctoral thesis
Swedish University of Agricultural Sciences
Uppsala 2005**

Acta Universitatis Agriculturae Sueciae
Agraria 504

ISSN 1401-6249
ISBN 91-576-6783-7
© 2004 Rosmarie Friemann, Uppsala
Tryck: SLU Service/Repro, Uppsala 2004

Abstract

Friemann, R., 2005, *Structure-Function Studies of Iron-Sulfur Enzyme Systems*.
Doctorial dissertation.
ISSN 1401-6249, ISBN 91-576-6783-7

Iron-sulfur clusters are among the most ancient of metal cofactors and serve a variety of biological functions in proteins, including electron transport, catalytic, and structural roles. Two kinds of multicomponent enzyme systems have been investigated by X-ray crystallography, the ferredoxin/thioredoxin system and bacterial Rieske non-heme iron dioxygenase (RDO) systems.

The ferredoxin/thioredoxin system is a light sensitive system controlling the activities of key enzymes involved in the assimilatory (photosynthetic) and dissimilatory pathways in chloroplasts and photosynthetic bacteria. The system consists of a ferredoxin, ferredoxin:thioredoxin reductase (FTR), and two thioredoxins, Trx-*m* and Trx-*f*. In light, photosystem I reduces ferredoxin that reduces Trx-*m* and Trx-*f*. This two-electron reduction is catalyzed by FTR that contains a [4Fe-4S] center and a proximal disulfide bridge. When the first electron is delivered by the ferredoxin, an intermediate is formed where one thiol of the proximal disulfide attacks the disulfide bridge of thioredoxin. This results in a transient protein-protein complex held together by a mixed disulfide between FTR and Trx-*m*. This complex is stabilized by using a C40S mutant Trx-*m* and its structure have been determined.

RDOs consists of a flavoprotein reductase and often a ferredoxin that transfer electrons from NAD(P)H to the terminal dioxygenase. The terminal dioxygenase catalyze the enantioselective addition of dioxygen in the initial degradation of aromatic compounds, producing *cis*-dihydrodiols. The structures of three dioxygenases, nitrobenzene dioxygenase (NBDO), 2-nitrotoluene (2NTDO) and toluene dioxygenase (TDO), as well as the two electron transfer proteins of the TDO system, toluene dioxygenase reductase (TDOR) and toluene dioxygenase ferredoxin (TDOF), have been determined. The dioxygenase structures are all $\alpha_3\beta_3$ heterohexamers similar to other RDOs. The catalytic α subunit contains a Rieske iron-sulfur cluster and a mononuclear iron at the active site. 2NTDO and NBDO are both able to degrade nitroaromatic compounds. Their structures and structures of NBDO in complex with two nitroarene substrates reveal the structural basis for the dihydroxylation of nitroarene compounds. The electron transfer pathway from NADH via TDOR and the TDOF to the TDO is described in relation to the obtained structures of the TDO system.

Keywords: Iron-sulfur protein, Rieske non-heme iron dioxygenase, ferredoxin thioredoxin:reductase, thioredoxin, nitroarene, X-ray crystallography

Author's address: Rosmarie Friemann, Department of Molecular Biology,
Swedish University of Agricultural Sciences, S-751 24 Uppsala, Sweden
E-mail: rosie@xray.bmc.uu.se

Contents

1. Introduction	9
2. Role of [4Fe-4S] cluster in reduction of disulfide bonds	11
2.1 Thioredoxin	11
2.1.1 Functions of thioredoxin	11
2.1.2 The thioredoxin fold	11
2.1.3 Mechanism of action	12
2.1.4 Reduction of thioredoxin	13
2.2 Structure of <i>Trypanosoma brucei brucei</i> thioredoxin (Paper I)	13
2.2.1 An unusual active site	13
2.3 The structure of ferredoxin: thioredoxin reductase– thioredoxin- <i>m</i> complex (Paper II)	15
2.3.1 The structures of the ferredoxin/thioredoxin system	15
2.3.1.1 Ferredoxin	15
2.3.1.2 FTR	17
2.3.1.3 Thioredoxin- <i>f</i> and Thioredoxin- <i>m</i>	17
2.3.2 Mechanism of action	17
2.3.3 The intermediate complex between FTR and Trx- <i>m</i>	19
3. Rieske non-heme iron dioxygenases	21
3.1 Organization and classification of Rieske non-heme iron dioxygenases	21
3.2 Structures of the components of the RDO systems	22
3.2.1 RDO reductases	22
3.2.2 RDO ferredoxins	23
3.2.3 RDOs	23
3.3 Mechanism of action	24
3.4 Structural studies of the electron transfer in the TDO enzyme system (Paper III & IV)	26
3.4.1 Crystallization and structure solution of the components of the TDO system	26
3.4.2 Structures of the components of the TDO system	27
3.4.2.1 TDOR	27
3.4.2.2 TDOF	27
3.4.2.3 TDO	28
3.4.2.4 apo-TDO	28
3.4.3 Electron transfer in the TDO system	29

3.5 The dioxygenation of nitroarene compounds (Paper V and VI)	31
3.5.1 Crystallization, data collection and structure solution of NBDO	32
3.5.2 Crystallization, data collection and structure solution of 2NTDO	33
3.5.3 Overall structures of NBDO and 2NTDO	34
3.5.4 Redox state of the Rieske center of NBDO	34
3.5.5 Comparison with other Rieske non-heme dioxygenases	34
3.5.6 Soaking and co-crystallization of NBDO with nitroaromatic compounds	35
3.5.7 Structures of NBDO in complex with nitrobenzene and 3-nitrotoluene	35
3.5.8 Substrate specificity of NBDO, 2NTDO NDO and DNTDO	36
4. Future perspectives	39
References	40
Acknowledgements	46

Appendix

Appendix A

Oxidation products formed by NBDO, 2NTDO, DNTDO and NDO

Appendix B

Table of data collection and refinement statistics for the structures mentioned in chapter 3.5

Appendix C

Sequence alignment of the C-terminal residues of the α subunit from NBDO, 2NTDO, DNTDO and NDO.

Papers I-VI

This thesis is based on the following papers, which will be referred to by their Roman numerals:

I. Friemann, R., Schmidt, H., Ramaswamy, S., Forstner, M., Krauth-Siegel, R.L., Eklund, H. (2003). Structure of thioredoxin from *Trypanosoma brucei*. *FEBS lett.* 554, 301-5.

II. Friemann, R., Eklund, H., Manieri W., Schürmann P., & Dai S. (2004). Structure of the ferredoxin: thioredoxin reductase-thioredoxin-*m* complex. *In manuscript.*

III. Lee, K., Friemann, R., Parales, J.V., Gibson D.T., & Ramaswamy S. (2004). Purification, crystallization and preliminary X-ray diffraction studies of the three components of the Toluene 2,3-dioxygenase enzyme system, (2004). *In manuscript.*

IV. Friemann, R., Lee, K., Gibson, D.T., Eklund, H., & Ramaswamy, S. (2004). Structural basis of electron transfer in the multicomponent Rieske non-heme Toluene 2,3-dioxygenase enzyme system. *In manuscript.*

V. Parales, R.E., Huang R., Yu, C.-L., Parales, J.V., Lee, F.K.N., Lessner, D.J., Ivkovic-Jensen, M.M., Liu, W., Friemann, R., Ramaswamy, S., & Gibson, D.T. (2004). Purification, characterization, and crystallization of the components of the Nitrobenzene and 2-Nitrotoluene enzyme systems. (2004). *Submitted, App. Environ. Microbiol.*

VI. Friemann, R., Ivkovic-Jensen, M.M., Lessner, D.J., Yu, C.-L., Gibson, D.T., Parales, R.E., Eklund, H., & Ramaswamy, S. (2004). Structural insight into the dioxygenation of nitroarene compounds: The crystal structure of Nitrobenzene dioxygenase. (2004). *Submitted, J. Mol. Biol.*

Paper I is reproduced by permission of the journal concerned.

Abbreviations

2,4-DNT	2,4-dinitrotoluene
2NT	2-nitrotoluene
3NT	3-nitrotoluene
4NT	4-nitrotoluene
2NTDO	2-nitrotoluene dioxygenase
AIF	apoptosis inducing factor
apo-TDO	toluene 2,3-dioxygenase apoenzyme
BphA1A2	biphenyl dioxygenase
BphA4	biphenyl dioxygenase reductase
BphF	biphenyl dioxygenase ferredoxin
DNTDO	2,4-dinitrotoluene dioxygenase
DTB	dethiobiotin
FBPase	fructose-1,6-bisphosphatase
FNR	ferredoxin- NADP reductase
FTR	ferredoxin: thioredoxin reductase
GR	glutathione reductase
MDH	malate dehydrogenase
NB	nitrobenzene
NBDO	nitrobenzene dioxygenase
NDO	naphthalene dioxygenase
NDOF	naphthalene dioxygenase ferredoxin
RDO	Rieske non-heme iron dioxygenase
RMS	root mean square
TDO	toluene 2,3-dioxygenase
TDOR	toluene 2,3-dioxygenase reductase
TDOF	toluene 2,3-dioxygenase ferredoxin
Trx- <i>f</i>	thioredoxin- <i>f</i>
Trx- <i>m</i>	thioredoxin - <i>m</i>
TrxR	NADPH thioredoxin reductase

1. Introduction

When life began approximately 3.5 - 4 billion years ago the atmosphere of early Earth constituted a reducing environment, with the most abundant gases, except water, being methane, carbon dioxide, nitrogen, and ammonia. Inorganic iron and sulfur, as a mixture of H₂S and FeS, were available in abundance and could readily combine with the first simple biomolecules, making iron-sulfur clusters among the most ancient of metallocofactors (Hall *et al.*, 1971).

Proteins containing iron-sulfur clusters play key roles in electron transport reactions, enzyme catalysis, and gene regulation (Beinert, 1997). The most common iron-sulfur clusters include [2Fe-2S], [3Fe-4S] and [4Fe-4S]. The iron ions are typically tetrahedrally coordinated by thiolate ligands of cysteine side chains with additional coordination to each iron provided by inorganic sulfides (Figure 1.1). Rubredoxin is one exception with its single iron center tetrahedrally coordinated by cysteines (Adman *et al.*, 1977). There are several examples of non-cysteinylligands to Fe-S clusters, including histidine ligation to [2Fe-2S] and [4Fe-4S] clusters (Volbeda *et al.*, 1995; Iwata *et al.*, 1996) and oxygen coordination to [4Fe-4S] clusters (Robbins and Stout, 1989).

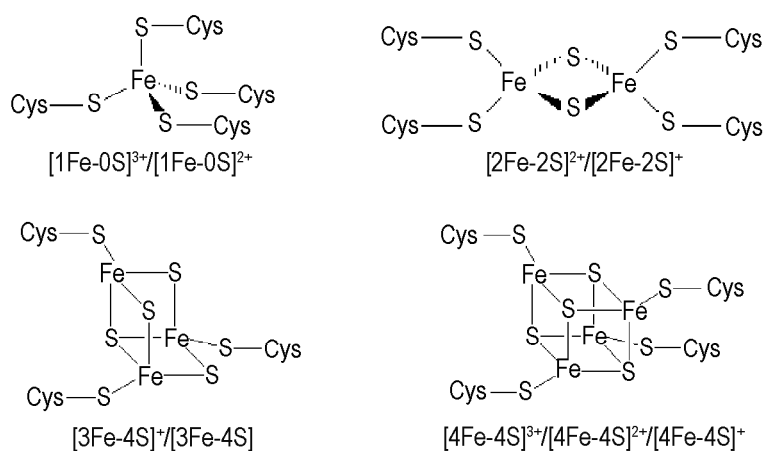


Figure 1.1. Examples of iron-sulfur clusters and their possible redox-states.

Iron-sulfur proteins have a diversity of functions, where electron transfer is the best studied. Ferredoxins are functionally and structurally the best characterized electron-transfer iron-sulfur proteins. They are small, ubiquitous soluble iron-sulfur proteins containing one or two iron-sulfur clusters of [2Fe-2S] or [4Fe-4S] type (Meyer, 2001).

This thesis comprises structure-function studies using X-ray crystallography of two different kinds of iron-sulfur multicomponent enzyme systems. These are the ferredoxin/thioredoxin system (Williams, 1992; Jacquot *et al.*, 1997) and the bacterial Rieske non-heme iron dioxygenase (RDO) systems (Gibson and Parales, 2000). In these systems the ferredoxins play an important role transferring electrons to their active sites. They contain a [2Fe-2S] cluster and are of two types: The cluster is either coordinated by four cysteines (plant-type) or by two cysteines and two histidines (Rieske-type).

The RDO enzyme systems consist of two or three soluble proteins, catalyzing the stereospecific addition of molecular oxygen in the initial degradation of aromatic hydrocarbons producing more soluble *cis*-dihydrodiols. Electrons are transferred from NAD(P)H via two or three iron-sulfur clusters to a mononuclear iron at the active site.

Iron-sulfur proteins are also involved in enzymatic reactions of no oxidoreductive nature, where iron-sulfur clusters directly participate in a catalytic process. Aconitase (citrate (isocitrate) hydroxylase) employs a [4Fe-4S] cluster to catalyze the stereospecific dehydration-rehydration of citrate to isocitrate via *cis*-aconitate in the tricarboxylic acid cycle (Robbins and Stout, 1989; Lloyd *et al.*, 1999).

Another fascinating example is biotin synthase, which catalyze the final step in the biotin biosynthetic pathway, the conversion of dethiobiotin (DTB) to biotin. The enzyme uses an [4Fe-4S] cluster and S-adenosyl-L-methionine to generate organic radicals for the insertion of a sulfur atom from a [2Fe-2S] cluster between two carbon atoms of DTB (Berkovitch *et al.*, 2004).

The FTR system is a light sensitive system controlling the activities of key enzymes involved in the assimilatory (photosynthetic) and dissimilatory pathways (Williams, 1992; Jacquot *et al.*, 1997) in chloroplasts and photosynthetic bacteria. The system consists of a [2Fe-2S] ferredoxin of plant type, ferredoxin:thioredoxin reductase (FTR) and two thioredoxin isoforms, Thioredoxin-*m* (Trx-*m*) and Thioredoxin-*f* (Trx-*f*). Photons captured by chlorophyll pigments in the photosystems are used to oxidize water and reduce the ferredoxin of the FTR system. FTR contains a [4Fe-4S] cluster and has a unique ability to reduce disulfide bridges through its iron-sulfur cluster via a non oxidoreductive reaction. It transforms the light signal, received in the form of electrons from the ferredoxin, into a thiol signal, which is then transmitted through disulfide-dithiol interchanges involving Trx-*m* and Trx-*f* to the target proteins.

2. Role of [4Fe-4S] cluster in reduction of disulfide bonds

2.1 Thioredoxin

The protein systems that are mainly responsible for the low redox potential and high free SH level inside the cells are the thioredoxin and the glutathione systems. Thioredoxins are small (approx. 12 kDa), ubiquitous redox active thiol proteins with a variety of important functions. Thioredoxin isoforms are present in most organisms, plants contain more types of thioredoxins than any other organism, and the mitochondria organelle has a separate thioredoxin.

2.1.1 Functions of thioredoxin

Thioredoxin has a large number of known functions and probably many more to be discovered. Some of them are described below but for a more comprehensive description the interested reader is recommended to look into several good reviews (Holmgren, 1985, 1995; Arner and Holmgren, 2000; Powis and Montfort, 2001 and references therein; Gromer *et al.*, 2004).

One of the earliest thioredoxin functions described was the donation of reducing equivalents to ribonucleotide reductase, which catalyzes the conversion of nucleotides to deoxynucleotides. Thioredoxins also serve as electron donors for thioredoxin peroxidases and methionine sulfoxide reductases.

Thioredoxins regulate enzymatic activities in chloroplasts and selectively activate the DNA-binding of a number of transcription factors, such as NF- κ B and p53. In addition mammalian thioredoxins have numerous functions in defence against oxidative stress, control of growth and apoptosis, but is also secreted and has co-cytokine and chemokine activities.

2.1.2 The thioredoxin fold

Extensive structural data exist for thioredoxin. Over 42 structures have been deposited in the protein data bank (Berman *et al.*, 2000). However, the structures from human and *E. coli* are the most thoroughly studied.

The typical thioredoxin structure consists of a five-stranded central β -sheet surrounded by four helices (Figure 2.1). The conserved active site amino acids, CGPC, link the second β strand to the second α helix, and form the first turn of this second helix. One of the catalytically redox active cysteine residues is buried, whereas the N-terminal active-site cysteine residue is more solvent exposed.

2.1.3 Mechanism of action

The catalytic efficiency of thioredoxins is based on the two redox-active Cys residues that undergo a two-electron oxidation to form a mixed disulfide bond. The N-terminal, solvent exposed active site Cys residue possesses a lower pK_a value than the more buried C-terminal active site Cys residue (Holmgren, 1995).

The proposed mechanism of thioredoxin-catalyzed protein disulfide reduction is shown in Figure 2.2. A nucleophilic attack by the thiolate of the N-terminal active site Cys residue breaks the disulfide bridge of the target protein, forming a disulfide bridge with the more electrophilic sulfur.

Thioredoxins have a conserved active site-buried Asp residue, which has been shown to act as a general acid/base catalyst towards the C-terminal active site Cys residue (Chivers and Raines, 1997; LeMaster *et al.*, 1997). The distance between this Cys and the Asp is large (approx. 6 Å) suggesting that protonation/deprotonation of the N-terminal active site Cys residue should be mediated by a water molecule (Menchise *et al.*, 2001). The transitory intermolecular disulfide bridge is then broken by the subsequent nucleophilic attack of the C-terminal active site Cys residue leaving the target protein reduced and releasing thioredoxin in the oxidized form.

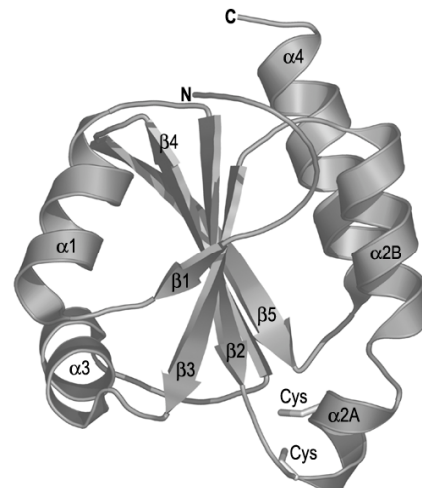


Figure 2.1. The overall structure of *Trypanosoma brucei* thioredoxin.

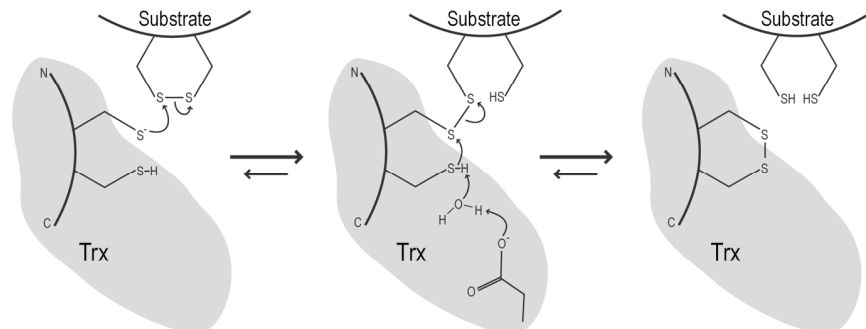


Figure 2.2 Proposed mechanism of thioredoxin-catalyzed protein disulfide reduction.

2.1.4 Reduction of thioredoxin

NADPH reduces all thioredoxin isoforms except the ones in photosynthetic bacteria and chloroplasts in a reaction catalyzed by the flavoprotein NADPH thioredoxin reductase (TrxR). TrxR uses an active site dithiol-disulfide to transfer reducing equivalents from NADPH via a FAD to the oxidized thioredoxin.

TrxRs can be divided in two classes, small TrxRs (approx. 35 kDa) and large TrxRs (approx. 55 kDa) (Gromer *et al.*, 2004). The small TrxRs are mainly found in bacteria but have also been identified in plants and fungi whereas the large TrxRs are mostly found in higher organisms and in mammals as a selenoenzyme.

In Chloroplasts and photosynthetic bacteria are thioredoxin reduced by ferredoxin thioredoxin:reductase (FTR), a unique enzyme that reduces disulfides by an iron-sulfur center. FTR will be discussed in greater detail in chapter 2.3

2.2 Structure of *Trypanosoma brucei brucei* thioredoxin (Paper I)

Trypanosomatids are the causative agents of several tropical diseases such as African sleeping sickness (*Trypanosoma brucei gambiense* and *Trypanosoma brucei brucei*), Nagana cattle disease (*Trypanosoma congolense* and *Trypanosoma brucei brucei*), and Chagas' disease (*Trypanosoma cruzi*).

These parasitic protozoa lack the glutathione system which is replaced by the trypanothione system, where the low molecular mass thiols trypanothione (N^1, N^8 -bis(glutathionyl)spermidine) and monoglutathionylspermidine are reduced by NADPH in a reaction catalyzed by trypanothione reductase (Fairlamb and Cerami, 1992; Krauth-Siegel and Coombs, 1999).

The properties of the unique trypanothione system and the failure to detect any thioredoxin reductase in trypanosomatids have led to the suggestion that these protozoa lack a thioredoxin system (Fairlamb and Cerami, 1992). Recently two thioredoxin sequences have been identified in the genome of *Leishmania major* and *Trypanosoma brucei brucei*, where the latter has been cloned, expressed and characterized (Myler *et al.*, 1999; Reckenfelderbäumer *et al.*, 2000). The *T. brucei* thioredoxin functions as an electron donor for *T. brucei* ribonucleotide reductase and is a substrate of human thioredoxin reductase but is not reduced by trypanothione reductase.

The structure of *T. brucei* thioredoxin was solved by molecular replacement using a polyalanine model of the reduced human thioredoxin. The overall structure is more similar to that of human thioredoxin than to any other known thioredoxin structure. The structure consists of a classical thioredoxin fold with a five-stranded central β -sheet surrounded by four helices (Figure 2.1).

2.2.1 An unusual active site

Interestingly a Trp residue in *T. brucei* thioredoxin replaces the highly conserved active site buried Asp residue (Figure 2.3). A water molecule is hydrogen bonded to the side chain nitrogen of this Trp residue.

Among the thioredoxin crystal structures containing an active site buried Asp, most structures have a water molecule hydrogen bonded to one of the oxygen atoms on the carboxylate. Superposition of the *Anabaena*, which has a Tyr at the corresponding position, human and *T. brucei* thioredoxin shows that the position of the water molecule hydrogen bonding to the side-chain of Trp in *T. brucei*, Asp in human thioredoxin corresponds to the position of the side-chain hydroxyl group of tyrosine in *Anabaena* thioredoxin (Figure 2.3).

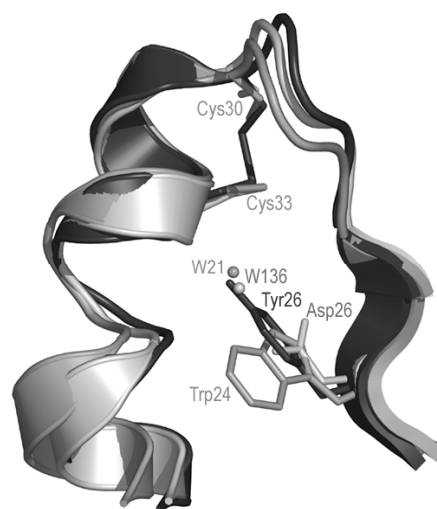


Fig. 2.3. Superposition of the active sites from *T. brucei* (dark gray), human (light gray) and *Anabaena* thioredoxin.

Since the side chain nitrogen of Trp is less electronegative than the side chain of Asp, the water that is believed to be involved in catalysis should be less polarized and not have the same possibilities to protonate/deprotonate the N-terminal active site Cys residue. Neighbouring residues may influence the pK_a of this water molecule. Lys57 in *E. coli* thioredoxin is close to the active site-buried Asp and has been shown to influence the catalytic efficiency (Dyson *et al.*, 1997). A double mutant of *E. coli* thioredoxin (D26A and K57M) reduced the catalytic activity even further than the D26A mutant. *T. brucei* has a Lys at the equivalent position, which is located 6 Å away from the water. The Lys side chain may swing down and come closer to the active site during catalysis, influencing the pK_a value of the water molecule.

2.3 The structure of the ferredoxin: thioredoxin reductase – Thioredoxin- *m* complex (Paper II)

Light is the primary energy source for metabolic activity in the chloroplast. During the day chloroplasts trap the energy from sunlight with their photosynthetic machinery to produce reducing equivalents, NADPH, and ATP, needed for the reduction of carbon dioxide to carbohydrates, which are then further used in the cellular metabolism as building blocks and an energy source.

During night time, however, chloroplast metabolism depends on stored energy. Catabolic processes break down storage products, like starch, accumulated in the chloroplasts during daylight to provide the necessary metabolic energy.

To avoid futile cycling, i.e. the simultaneous functioning of assimilatory and dissimilatory pathways, the two processes are strictly controlled by a light-dependent mechanism (Buchanan, 1980, 1991; Scheibe, 1994; Jacquot *et al.*, 1997; Schürmann and Buchanan, 2001; Buchanan *et al.*, 2002).

The signal for this light/dark control is light. Light, sensed by the thylakoid pigments, acts through a redox-signaling cascade known as the ferredoxin/thioredoxin system. This system involves ferredoxin, ferredoxin:thioredoxin reductase (FTR), thioredoxin-*m* (Trx-*m*) and thioredoxin-*f* (Trx-*f*), the latter being absent in cyanobacteria (Schürmann, 2003). Electrons needed for the reductions are provided by the photosynthetic light reactions and relayed by ferredoxin to FTR. This enzyme, unique to oxygenic photosynthetic cells, transforms the light signal, received in the form of electrons, into a thiol signal, which is then transmitted through disulfide-dithiol interchanges involving thioredoxins to the target proteins.

2.3.1 The structures of the ferredoxin/thioredoxin system.

In recent years the structures of photosystem I, the components of the ferredoxin/thioredoxin system and of two well studied target enzymes, malate dehydrogenase (MDH) and fructose 1,6-bisphosphatase (FBPase) have been solved. (Figure 2.4) (Villeret, 1995; Carr *et al.*, 1999; Chiadmi *et al.*, 1999; Johansson *et al.*, 1999; Capitani *et al.*, 2000; Dai *et al.*, 2000a; Dai *et al.*, 2000b; Jordan *et al.*, 2001; Antonkine *et al.*, 2003).

2.3.1.1 Ferredoxin

The [2Fe-2S] cluster of ferredoxin is reduced by a [4Fe-4S] cluster located in the PsaC subunit of photosystem I. Several three-dimensional structures of plant-type ferredoxins share the same fold with a five stranded β -sheet, two to three α -helices and a long loop. The [2Fe-2S] center is attached towards the outer edge of the molecule by four cysteine ligands in the long loop.

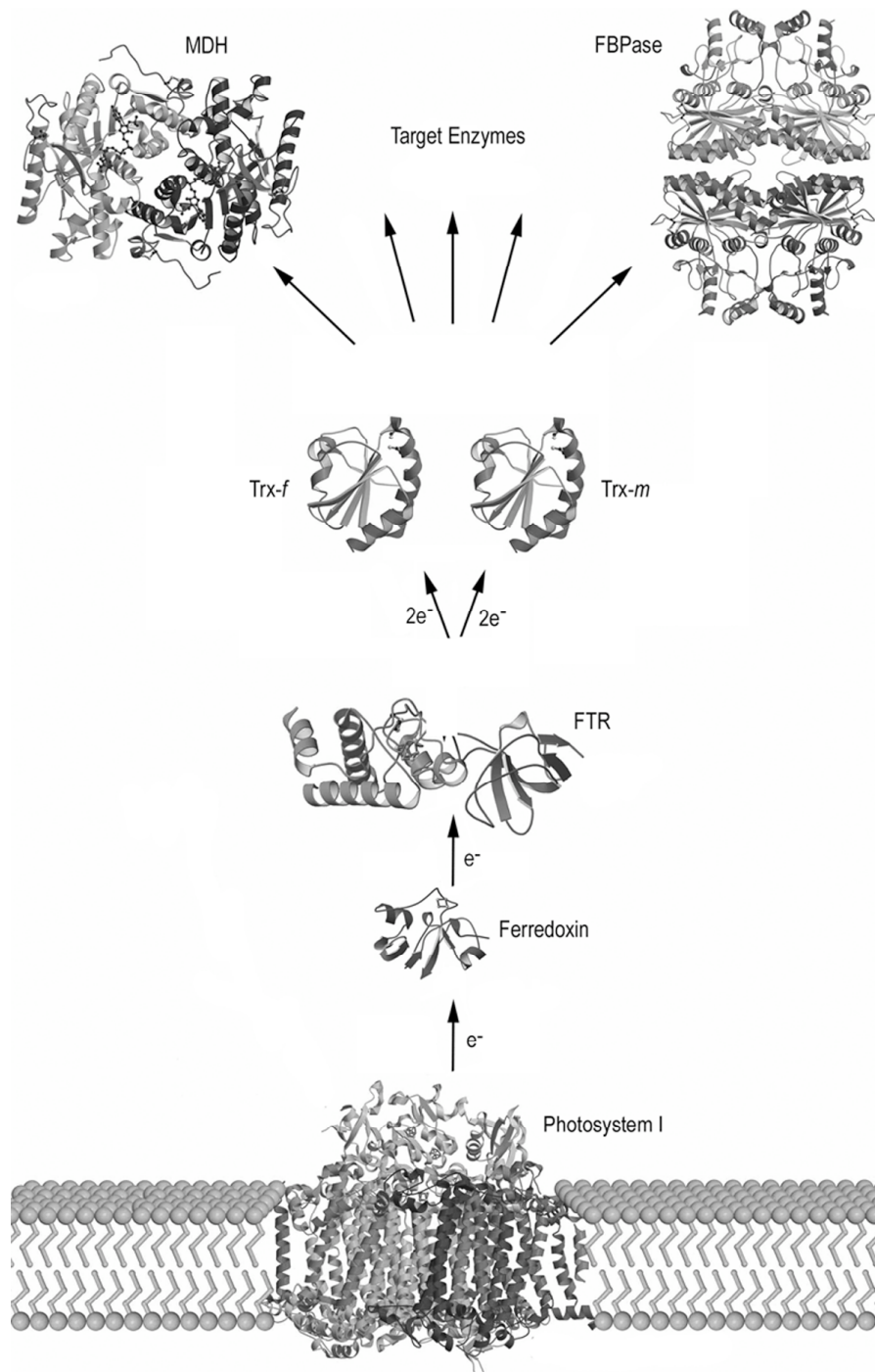


Figure 2.4. Electrons are transferred from photosystem I via ferredoxin to FTR. In order to reduce a thiooxidin, FTR need two electrons from two ferredoxin molecules. The thiooxidins can then reduce disulfides in target enzymes, exemplified by malate dehydrogenase (MDH) and fructose 1,6-bisphosphatase (FBPase).

2.3.1.2 Ferredoxin:thioredoxin reductase

FTR transduces the general redox-signal from the one-electron donor ferredoxin to thioredoxins, which are two-electron donors. FTR utilizes a [4Fe-4S] cluster and a disulfide bridge close to this cluster to mediate electron transfer in two steps from ferredoxin to cleave disulfide bridges of thioredoxin. FTR is a $\alpha\beta$ -heterodimer composed of a 13 kDa catalytic subunit and a variable subunit of similar or smaller size. The variable subunit is an open β -barrel structure consisting of five antiparallel strands. The catalytic subunit, mainly an α -helical structure, contains the redox-active disulfide and the [4Fe-4S] center coordinated by four cysteines.

2.3.1.3. Thioredoxin-*f* and Thioredoxin-*m*

The chloroplast thioredoxins show the typical thioredoxin fold with a central, twisted, five-stranded β -sheet surrounded by four α -helices. The Trx-*f* contains an additional N-terminal α -helix. The significant difference between Trx-*f* and Trx-*m* is the surface topology and charge distribution around the active site, influencing the specificity towards target enzymes. Trx-*f* contains a third conserved cysteine residue, which is surface exposed approximately 10 Å away from the active site cysteines. Trx-*f* displays a high specificity towards FBPase and several other Calvin cycle enzymes as well as rubisco activase, the ATP synthase CF1 complex, and MDH. Trx-*m* is only known to interact specifically with fructose 6-phosphate dehydrogenase. Unlike the other target enzymes, fructose 6-phosphate dehydrogenase is inactivated by the Trx-*m* reduction, thereby stopping the oxidative pentose phosphate cycle in the light.

2.3.2 Mechanism of action

In FTR the iron-sulfur cluster is able to reduce disulfides due to its close proximity to an active site disulfide bridge. When the first ferredoxin delivers one electron to the [4Fe-4S]²⁺ cluster it will not result in a reduction of the cluster. Instead the electron from the ferredoxin and one electron from the iron-sulfur cluster of FTR are used to cleave the active site disulfide bridge leaving the cluster in the oxidized [4Fe-4S]³⁺ state (Figure 2.5). In this intermediary state, labelling has shown that only one of the cysteines, Cys57, is a reactive thiol while the second cysteine, Cys87, is protected by the iron-sulfur cluster (Staples *et al.*, 1996). Initially this intermediate was thought to have a disulfide bridge formed between the cysteine and a sulfide ion in the iron-sulfur cluster (Staples *et al.*, 1996). However, in the structure of FTR, Cys87 has a tight interaction to one of the iron atoms of the cluster, which led to the suggestion the Cys coordinates the iron in the intermediate stage forming a penta-coordinated iron (Dai *et al.*, 2000b). Such a structure is also supported by recent Mössbauer studies on FTR (Jameson *et al.*, 2003).

In the second step a transient heterodisulfide is formed between the FTR and thioredoxin by the nucleophilic attack of Cys57 on the disulfide of thioredoxin. In a third step the second electron delivered by a second ferredoxin molecule to the iron-sulfur center reduces it back to its original 2^+ oxidation state while Cys87 becomes a nucleophilic thiol that can attack the heterodisulfide bridge between FTR and thioredoxin and thereby release the fully reduced thioredoxin in the fourth step.

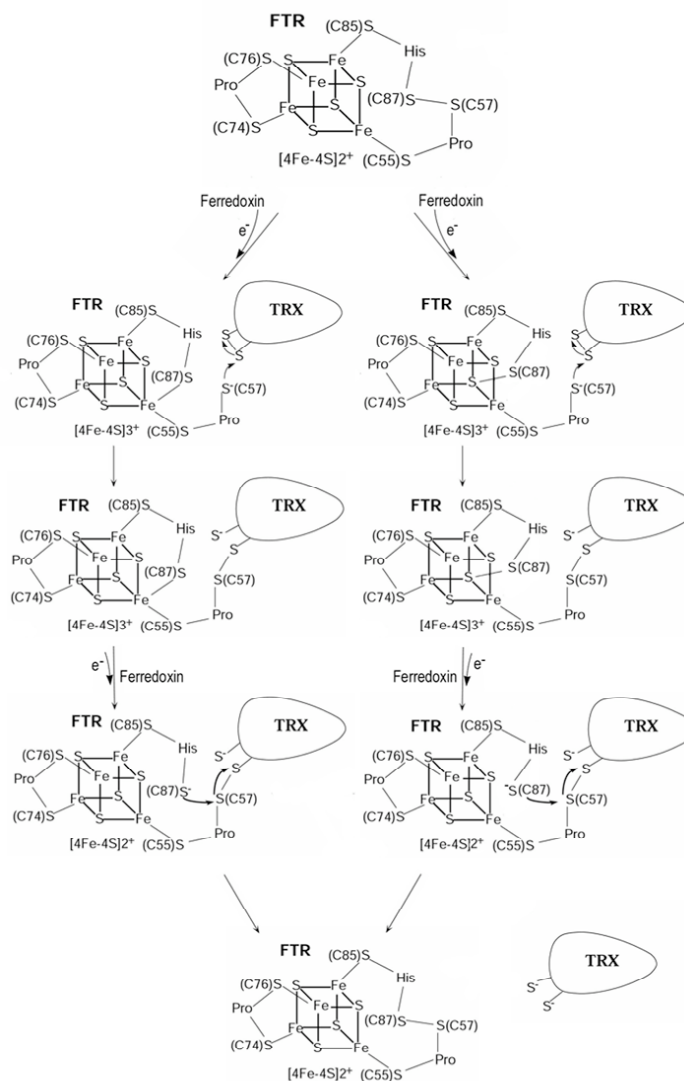


Figure 2.5. Proposed mechanism of action according to Staples (right path) and Dai (left path).

2.3.3 The intermediate complex between FTR and Trx-*m*

By mutating the buried C-terminal active site Cys residue of thioredoxin, the intermediate intermolecular disulfide bridge between thioredoxin and FTR is stabilized. To elucidate the interplay and mechanism of FTR, i.e. if Cys87 forms a penta-coordinated iron or a disulfide bridge to a sulfide ion of the iron-sulfur cluster in the intermediate stage, the structure of a complex between FTR and mutant Trx-*m* C40S has been determined to 3.0 Å resolution.

The overall structure is illustrated in Figure 2.6. Thioredoxin is positioned on the side of the thin, concave, disk-shaped FTR molecule, exclusively interacting with the catalytic domain. This is also seen in the structures of the FTR-Trx-*f* and ferredoxin-FTR complexes (Dai, unpublished). The role of the variable subunit is not known. Interestingly the structure of the variable domain is similar to the GroES type chaperone subunit (Hunt, 1997) (RMS deviation of 1.61 Å for 44 C α atoms). The variable domain of FTR could stabilize the structure of the catalytic subunit or have a chaperon like function.

A disulfide bridge between the solvent exposed active site cysteine of Trx-*m* and Cys57 of FTR covalently links the two molecules, resembling the intermediate in the reaction (Figure 2.7). In the third step of the reaction (Figure 2.5) a second electron is delivered to the iron-sulfur cluster by a second ferredoxin molecule. In the structure of the ferredoxin-FTR complex (Dai, unpublished) the ferredoxin molecule interacts on the opposite side of FTR from the thioredoxin binding site.

Except for the intermolecular disulfide, there are very few interactions between the proteins in the FTR-Trx-*m* complex. The conserved active site Trp and Gly residues of Trx-*m* are in van der Waals contact with residues of FTR. The side-chain conformation of the conserved Trp is in most thioredoxin structures covering the surface of the molecule. However, in the FTR-Trx-*m* complex the Trp is flipped out from the thioredoxin molecule interacting with FTR. This flipped conformation of the Trp residue was also observed in the *T. brucei* thioredoxin and a few other cases (Nikkola, 1991; Capitani *et al.*, 2000; Friemann *et al.*, 2003).

The main interactions between Trx-*m* and FTR are located around residues 73-81 of Trx-*m* and residues 57-61 of the catalytic domain of FTR (residues 57-60 of the catalytic domain of FTR are completely conserved), where there are several hydrogen bonds between the proteins molecules (Figure 2.8).

Finally, the FTR-Trx-*m* intermediate structure reveals that Cys87 of the catalytic subunit of FTR forms the fifth ligand to an iron atom in the cluster, suggesting that the mechanism of action is as described by Dai *et al.* Higher resolution data is necessary to resolve the detailed cluster geometry.

In the final step of the reaction Cys87 is released from the iron-sulfur center when the second ferredoxin reduces the cluster. In order to attack Cys57 of the intermolecular disulfide bond, Cys87 only needs to rotate about 30° around the C α -C β bond to be in the perfect position for the nucleophilic attack.

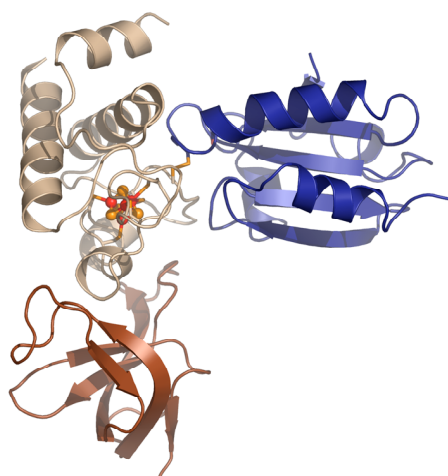


Figure 2.6. Overall structure of the FTR-Trx-*m* complex. Trx-*m*, catalytic- and variable domains of FTR are shown in blue, beige and brown.

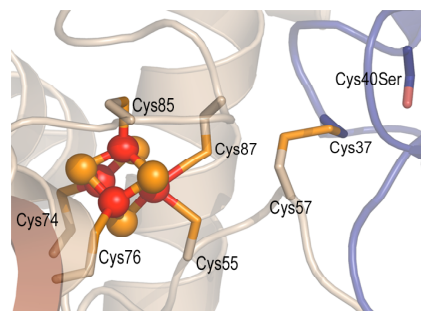


Figure 2.7. The active sites of FTR (beige) and Trx-*m* (blue) are linked by a disulfide bridge, resembling the intermediate of the reaction. Cys87 interacts with the [4Fe-4S] cluster forming a five-coordinated iron atom.

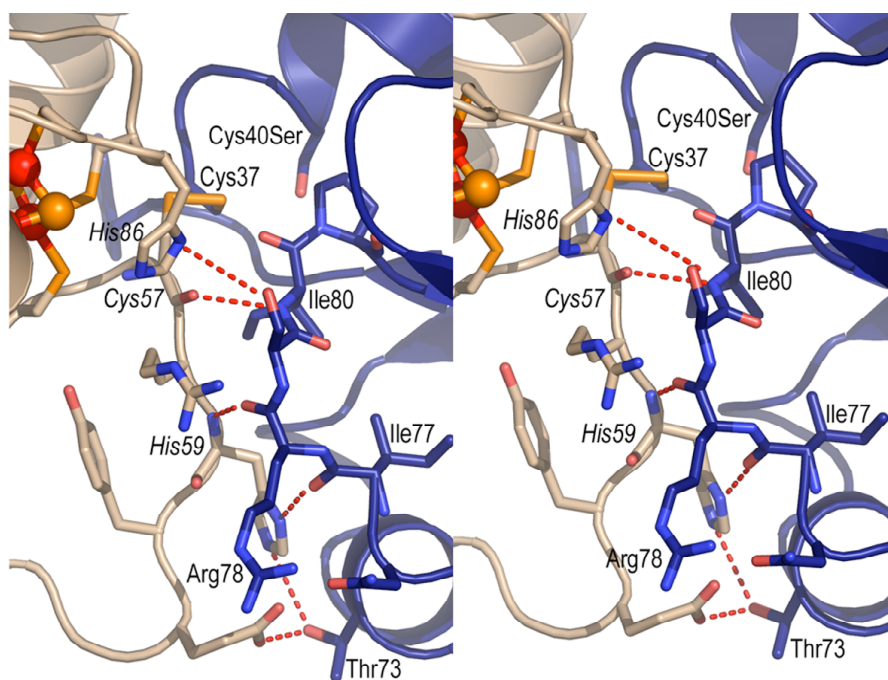


Figure 2.8. Interactions between the catalytic subunit of FTR (beige) and Trx-*m* (blue). Labels for FTR amino acids are shown in italics.

3. Rieske non-heme iron dioxygenases

Many aromatic compounds are considered toxic, mutagenic, and carcinogenic (Daly JW, 1972). The use of petroleum products for fuel and the manufacture of plastics, pharmaceuticals, herbicides, pesticides, cosmetics, and other chemicals has led to an excessive production of aromatic compounds, resulting in environmental pollution of soils and groundwaters.

Several bacteria that degrade aromatic compounds contain a multicomponent Rieske non-heme iron dioxygenase (RDO) enzyme system that catalyzes the incorporation of both atoms of molecular oxygen into the aromatic ring to yield an arene *cis*-diol. In the course of the reaction one dioxygen, two electrons and two protons are consumed. A flavo NAD(P)H reductase, and sometimes a ferredoxin, transport electrons to the dioxygenase which catalyzes the reaction. At present, more than thirty RDO systems have been identified, producing over 300 vicinal arene *cis*-diols as the reaction products of aromatic hydrocarbons. In almost all cases, the arene *cis*-diols produced are single enantiomers (Resnick *et al.*, 1996; Boyd and Sheldrake, 1998; Hudlicky *et al.*, 1999).

Bacterial strains that are able to degrade environmentally hazardous aromatic compounds may be useful for the development of bioremediation technologies for the clean up of contaminated environments (Lau and De Lorenzo, 1999). In addition, the fact that RDOs have broad substrate ranges and many products are enantiomerically pure compounds that are difficult to generate using standard chemical synthesis could make them useful in the fields of asymmetric synthesis and “green chemistry” (Sheldrake, 1992; Hudlicky and Reed, 1995; Boyd and Sheldrake, 1998; Hudlicky *et al.*, 1999; Anastas and Kirchhoff, 2002).

3.1 Organization and classification of Rieske non-heme iron dioxygenases

RDO systems consist of two or three soluble proteins that interact to form an electron-transport chain that transfers electrons from reduced nucleotides (NAD(P)H) via flavin and [2Fe-2S] redox centers to a terminal dioxygenase (Table 3.1) (Batie *et al.*, 1991; Gassner *et al.*, 1995). The two component RDO systems hold a reductase, containing a flavin and [2Fe-2S] center of plant type, and a terminal dioxygenase. In the three component systems, the electrons are transferred from the reductase to the dioxygenase via a ferredoxin of plant or Rieske type. The reductases contain a flavin and sometimes a Rieske [2Fe-2S] center. The dioxygenases are heteromultimers consisting of α and β subunits, where the α subunits contain a Rieske [2Fe-2S] cluster and mononuclear iron.

Gibson and Parales recently suggested classifying the RDOs into four dioxygenase families based on their native substrate and the amino acid sequence of their respective α subunit. These families are Naphthalene, Toluene/Biphenyl, Benzoate and Phthalate (Table 3.2).

Table 3.1 Organization of RDO systems (Batie *et al.*, 1991; Gassner *et al.*, 1995). The [2Fe-2S] centers are represented as P or R for plant- or Rieske type ferredoxins respectively.

	Reductase	Ferredoxin	Oxygenase	Examples
Two component systems	FMN [2Fe-2S] _P	-	[2Fe-2S] _R Fe ²⁺	Phthalate dioxygenase
	FAD [2Fe-2S] _P	-	[2Fe-2S] _R Fe ²⁺	Benzoate dioxygenase
Three component systems	FAD	[2Fe-2S] _P	[2Fe-2S] _R Fe ²⁺	Dibenzofuran dioxygenase
	FAD	[2Fe-2S] _R	[2Fe-2S] _R Fe ²⁺	Toluene dioxygenase Biphenyl dioxygenase
	FAD [2Fe-2S] _R	[2Fe-2S] _R	[2Fe-2S] _R Fe ²⁺	Naphthalene dioxygenase Nitrobenzene dioxygenase 2-Nitrotoluene dioxygenase

Table 3.2 The RDO families.

Dioxygenase Family	Examples of dioxygenases and compounds degraded
Naphthalene	Naphthalene, phenanthrene, nitrobenzene, nitrotoluene
Toluene/Biphenyl	Toluene, benzene, isopropylbenzene, chlorobenzenes, biphenyl
Benzoate	Benzoate, toluate, anthranilate, 2-chlorobenzoate, trichlorophenoxyacetate, isopropylbenzoate
Phthalate^a	Vanillate, phthalate, 3-chlorobenzoate, phenoxybenzoate, p-toluene sulfonate

^aThe Phthalate family contains both dioxygenases and monooxygenases.

3.2 Structures of the components of the RDO systems

3.2.1 RDO reductases

The RDO reductases belong to either the ferredoxin-NADP reductase (FNR) family or the glutathione reductase (GR) family. Structures of FNR-type are phthalate dioxygenase reductase (Correll *et al.*, 1992) and benzoate 1,2-dioxygenase (Karlsson *et al.*, 2002). These FNR reductases (approx. 36 kDa) consist of a NADH binding domain, a FAD- or FMN-binding domain and a ferredoxin like domain containing a plant-type [2Fe-2S] center.

Known structures of GR-type are biphenyl dioxygenase reductase (BphA4) (Senda *et al.*, 2000) and Toluene dioxygenase reductase (TDOR) (paper IV). BphA4 and TDOR (approx. 43 kDa) are three-domain proteins consisting of a NADH-binding domain, a FAD binding domain and a C-terminal domain, corresponding to the interface domain of GR. The structure of TDOR is further described in section 3.4.2.1 and paper IV.

3.2.2 RDO ferredoxins

The RDO ferredoxins (approx. 12 kDa) contain an [2Fe-2S] center of plant- or Rieske-type. Currently three ferredoxin structures of Rieske-type have been determined, biphenyl dioxygenase ferredoxin (BphF) (Colbert *et al.*, 2000), naphthalene dioxygenase ferredoxin (NDOF) (Karlsson, 2002) and toluene dioxygenase ferredoxin (TDOF) (paper IV). The ferredoxins are elongated molecules dominated by three antiparallel β sheets with the Rieske center located at the tip of the molecule. The structure of TDOF is described in greater detail in section 3.4.2.2 and paper IV.

3.2.3 RDOs

RDOs are mushroom shaped $\alpha_3\beta_3$ hetero-hexamers (approx. 220 kDa) as seen in naphthalene dioxygenase (NDO) (Kauppi *et al.*, 1998), biphenyl dioxygenase (BphA1A2) (Furusawa *et al.*, 2004), nitrobenzene dioxygenase (NBDO) (paper VI), 2-nitrotoluene dioxygenase (2NTDO) (section 3.5) and toluene 2,3-dioxygenase (TDO) (paper IV). The cap and stem are composed of the α_3 and β_3 subunits respectively (Figure 3.1).

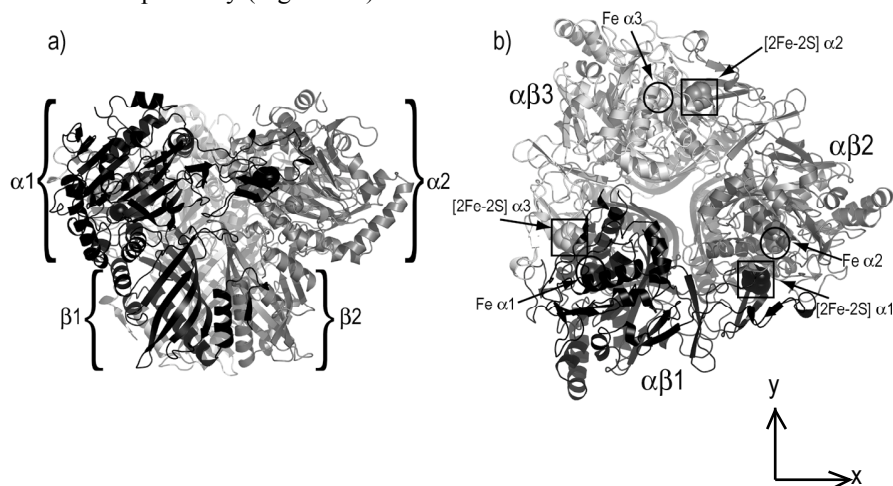


Figure 3.1. Overall structure of NBDO. b) is a 90° rotation around the X-axis of a).

The β subunit has most probably a structural role (Tan and Cheong, 1994; Beil *et al.*, 1998; Parales *et al.*, 1998a; Parales *et al.*, 1998b; Jiang *et al.*, 1999) and consists of a long twisted six-stranded mixed β -sheet. The pleated sheet has three helices on the concave side and one N-terminal helix on the convex side. The general three-dimensional structure of the β subunit is similar to a number of other functionally unrelated proteins: the association domain of Ca^{2+} /Calmodulin-dependent protein kinase II (Hoelz *et al.*, 2003), scytalone dehydratase (Lundqvist *et al.*, 1994), nuclear transport factor 2 (Bullock *et al.*, 1996), Δ^5 -3-ketosteroid isomerase (Kim *et al.*, 1997), the N-terminal domain of penicillin binding protein 2a (Lim and Strynadka, 2002), limonene-1,2-epoxide hydrolase (Arand *et al.*, 2003) and the C-terminal domain of orange carotenoid protein (Kerfeld *et al.*, 2003).

The α subunit has a Rieske domain that contains a Rieske [2Fe-2S] center, and a catalytic domain that contains mononuclear iron at the active site. The mononuclear iron is coordinated by two histidines and an aspartate.

The Rieske domain is dominated by three antiparallel β -sheets and is very similar to the RDO ferredoxins (Colbert *et al.*, 2000; Karlsson, 2002), the Rieske subunit of arsenite oxidase (Ellis *et al.*, 2001), the Rieske domains of cytochrome bc_1 (Iwata *et al.*, 1996; Iwata *et al.*, 1998), cytochrome b_6f (Carrell *et al.*, 1997) and the respiratory-type Rieske protein (Hunsicker-Wang *et al.*, 2003).

The catalytic domain consists of a nine-stranded antiparallel β -sheet surrounded by twelve α helices. The structure of the domain belongs to the helix-grip fold (Iyer *et al.*, 2001) and resembles birch pollen allergen protein Betv1 (Gajhede *et al.*, 1996), the multifunctional phosphatidylinositol transfer protein (Yoder *et al.*, 2001), steroidogenic acute regulatory protein related lipid transfer (StAR) domain MLN64 (Tsujishita and Hurley, 2000) and the cholesterol-regulated START protein 4 (StarD4) (Romanowski *et al.*, 2002).

The structures of NBDO and 2NTDO are further described in chapter 3.5 and paper VI, TDO in chapter 3.4 and paper IV, respectively.

3.3 Mechanism of action

NDO is the RDO that has been most thoroughly studied. It catalyzes a wide variety of reactions including mono/di-hydroxylation, desaturation, *O*- and *N*-dealkylation and sulfoxidation reactions (Resnick *et al.*, 1996).

The dihydroxylation reaction requires one dioxygen, two protons and four electrons. Two of the electrons are transferred from NAD(P)H, while the other two are provided from a double bond of the aromatic substrate. Figure 3.2 shows a schematic representation of the electron transfer pathway from NADH to the mononuclear iron at the active site in the TDO enzyme system. Initially, two electrons are transferred from NAD(P)H to a flavin in the reductase. Electrons are then transferred one at a time from the reductase to the Rieske center of the ferredoxin. The ferredoxin shuttles the electron via the dioxygenase Rieske center of one α subunit to the mononuclear iron in the neighbouring subunit through a hydrogen bonded system containing a conserved aspartic acid (Kauppi *et al.*, 1998; Parales *et al.*, 2000a).

The catalytic mechanism of dioxygen activation yielding *cis*-dihydroxylation of the substrates in RDO's is still elusive. Recently S.A. Karlsson *et al.*, (2003) determined structures of NDO with substrates, oxygen, substrate plus oxygen, and product. Interestingly, molecular oxygen is bound to the mononuclear iron in a side-on fashion, which suggests a concerted mechanism where both oxygen atoms react with the carbon atoms of the substrate double bond (Figure 3.3).

The dioxygen reaction takes place only when the dioxygenase Rieske center and the active site iron are in the reduced form as demonstrated for NDO (Wolfe *et al.*, 2001). It was further shown that during single turnover, both the mononuclear iron and the Rieske center were oxidized. The intermediate of the reaction might be a peroxy-iron(III) or a hydro-peroxy-iron(III), where the latter is supported by a hybrid density functional theory study (Bassan *et al.*, 2004). The hydroxylated product is formed and a second electron delivered by ferredoxin reduces the mononuclear iron.

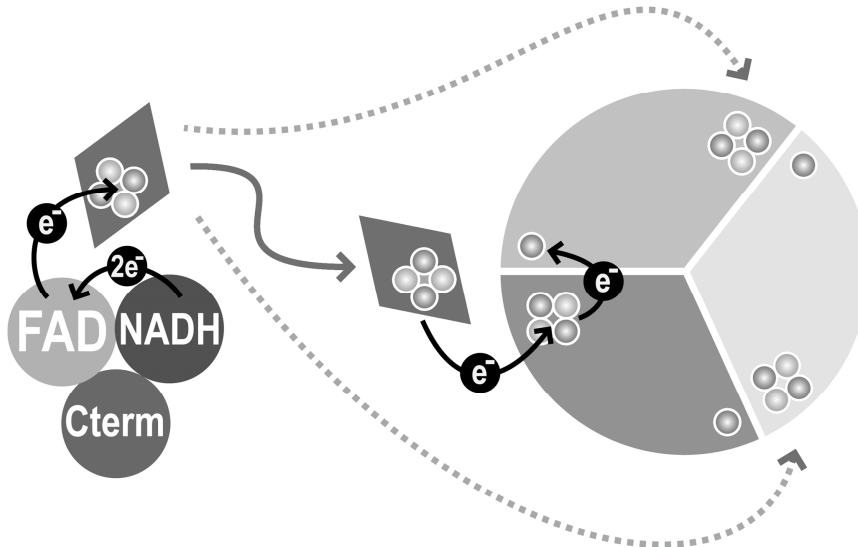


Figure 3.2. Schematic representation of the electron transfer pathway in the TDO enzyme system. Two electrons are transferred from NADH to FAD in the reductase. The ferredoxin (shown as a rhombus) shuttle one electron from FAD via the dioxygenase Rieske center to the mononuclear iron in the neighbouring subunit.

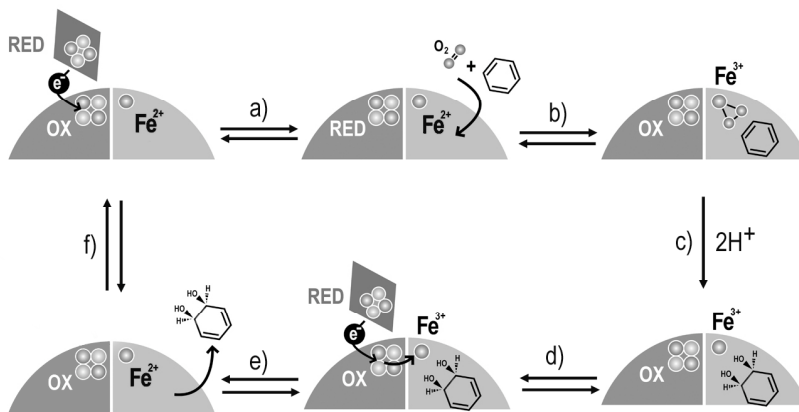


Figure 3.3. Proposed mechanism of dihydroxylation by RDO.

3.4 Structural studies of the electron transfer pathway in the TDO enzyme system (Paper III & IV).

Toluene is extensively used as a gasoline component and an industrial solvent that has led to pollution of soils, groundwaters and urban atmospheres (Greenberg, 1997). *Pseudomonas putida* F1, can grow with toluene as its sole source of carbon and energy, where the initial degradation is catalyzed by the three-component TDO enzyme system consisting of a reductase (TDOR), ferredoxin (TDOF) and toluene 2,3-dioxygenase (TDO) (Gibson *et al.*, 1968). TDO catalyzes the enantioselective addition of dioxygen to toluene to form *cis*-(1*R*,2*S*)-dihydroxy-3-methylcyclohexa-3,5-diene (*cis*-toluene dihydrodiol) (Gibson *et al.*, 1970; Kobal *et al.*, 1973) (Figure 3.4).

In order to gain insights into the electron transfer chain, structures of all the components in the TDO system have been determined.

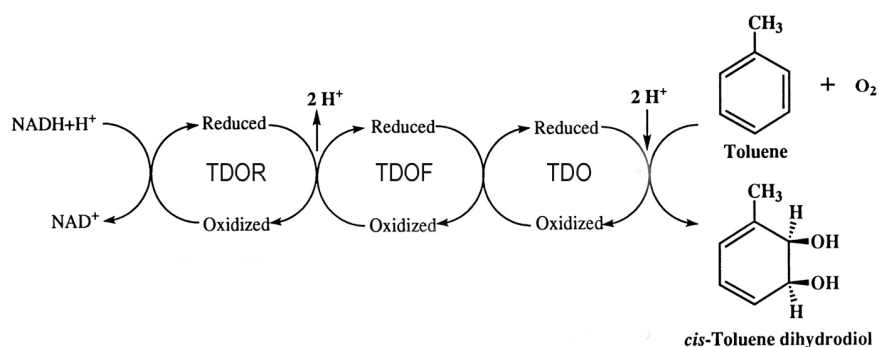


Figure 3.4. Dihydroxylation of toluene to *cis*-toluene dihydrodiol, catalyzed by the three-component TDO system.

3.4.1 Crystallization and structure solution of the components of the TDO system

The components of the TDO system were crystallized by the vapor-diffusion method. The mononuclear iron in TDO is not strongly bound and is lost during purification. TDO without mononuclear iron is referred to TDO as apoenzyme (apo-TDO). The reconstitution of the mononuclear iron was performed by co-crystallization with ferrous ammonium sulfate in an anaerobic box.

TDOR, TDOF, apo-TDO and TDO diffracted to 1.8 Å, 1.2 Å, 3.2 Å and 3.2 Å respectively. The structures of the components were solved by molecular replacement using components from different Biphenyl dioxygenase systems (Colbert *et al.*, 2000; Senda *et al.*, 2000; Furusawa *et al.*, 2004).

3.4.2 Structures of the components of the TDO system

3.4.2.1 TDOR

TDOR has a GR fold and can be divided into three domains: a FAD-binding domain, NADH-binding domain and C-terminal domain (Figure 3.5). The FAD-binding domain has a five-stranded parallel β -sheet and the NADH-binding domain has a four-stranded parallel β -sheet. In both domains there are three α -helices on either side of the sheet and a three-stranded β -meander on the other side. The C-terminal domain consists of a five-stranded antiparallel β -sheet with two α -helices and one 3_{10} helix on the C-terminal side of the sheet. The FAD molecule binds non-covalently through a cleft in the FAD binding

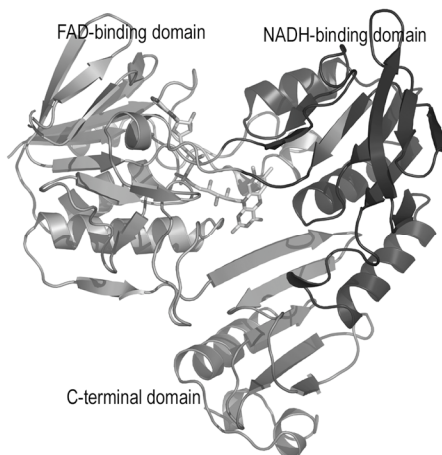


Figure 3.5. Overall structure of TDOR.

domain in an extended conformation. Extensive hydrogen bonding from 10 water molecules and the main- and side-chains of 11 residues hold the FAD in position. TDOR is similar to the GR-family enzymes (Schulz *et al.*, 1978; Karplus and Schulz, 1989) and shares the highest structural similarity with biphenyl dioxygenase reductase (BphA4) (Senda *et al.*, 2000) and the mammalian apoptosis inducing factor (AIF) (Mate *et al.*, 2002; Ye *et al.*, 2002).

3.4.2.2 TDOF

TDOF is an elongated molecule dominated by three antiparallel β -sheets (A, B and C) (Figure 3.6). A Rieske [2Fe-2S] center is located at the tip of the molecule, where the ligating histidines are exposed to the surface of the molecule. The ferredoxin structure is very similar to biphenyl dioxygenase ferredoxin (BphF) (Colbert *et al.*, 2000) and NDO ferredoxin (NDOF) (Karlsson, 2002) as well as the Rieske domain of RDOs and other Rieske iron-sulfur domains (summarized in chapter 3.2.3).

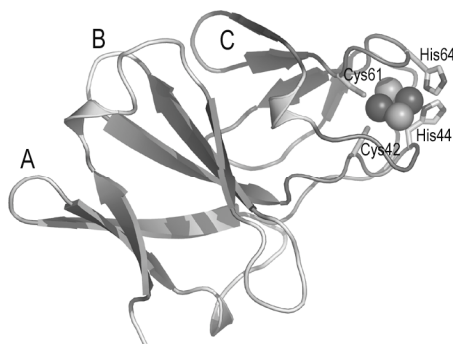


Figure 3.6. Overall structure of TDOF

3.4.2.3 TDO

TDO is composed of an $\alpha_3\beta_3$ hetero-hexamer as found in the known structures of RDOs. The α subunit has a Rieske domain that contains a Rieske [2Fe-2S] center and a catalytic domain that contains mononuclear iron at the active site, coordinated by two His and one Asp. Among RDOs, TDO shares the highest structural similarity with biphenyl dioxygenase (BphA1A2) (Furusawa *et al.*, 2004). Both enzymes belong to the Biphenyl/Toluene dioxygenase family and share a 77 % sequence identity. The substrate binding pocket is lined by 17 mainly hydrophobic residues, where only one residue differs between TDO and BphA1A2 (Val309 in TDO, Ala311 in BphA1A2). Both TDO and BphA1A2 oxidizes biphenyl to *cis*-(1*S*,2*R*)-dihydroxy-3-phenylcyclohexa-3,5-diene. In the absence of rigorous substrate selectivity studies in BphA1A2 the effect on substrate specificity on a single amino acid change will be hard to predict.

3.4.2.4 apo-TDO

The loss of the mononuclear iron causes conformational changes in both subunits. An α -helix containing one of the iron ligands (His222) becomes disordered in the apo-structure (Figure 3.7). The main-chain oxygen of Thr226 of the α subunit hydrogen bonds to the side chain of Trp211 of the β subunit in TDO. Due to the flexibility in the α -helix containing His222, Thr226 is positioned differently leading to a conformational change in the area around Trp211 of the β subunit.

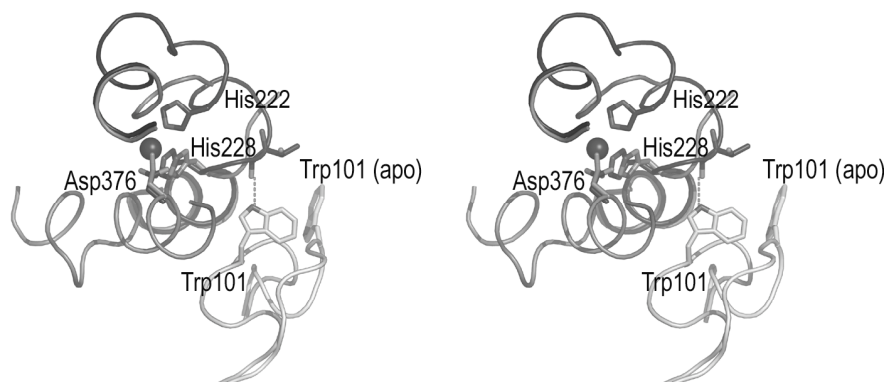


Figure 3.7. Comparison of TDO and apo-TDO. The α subunit is shown in dark gray (TDO) and light gray (apo-TDO). The β subunit is shown in white.

3.4.3 Electron transfer in the TDO system

Electrons are transferred from NADH to the mononuclear iron at the active site in TDO via TDOR and TDOF.

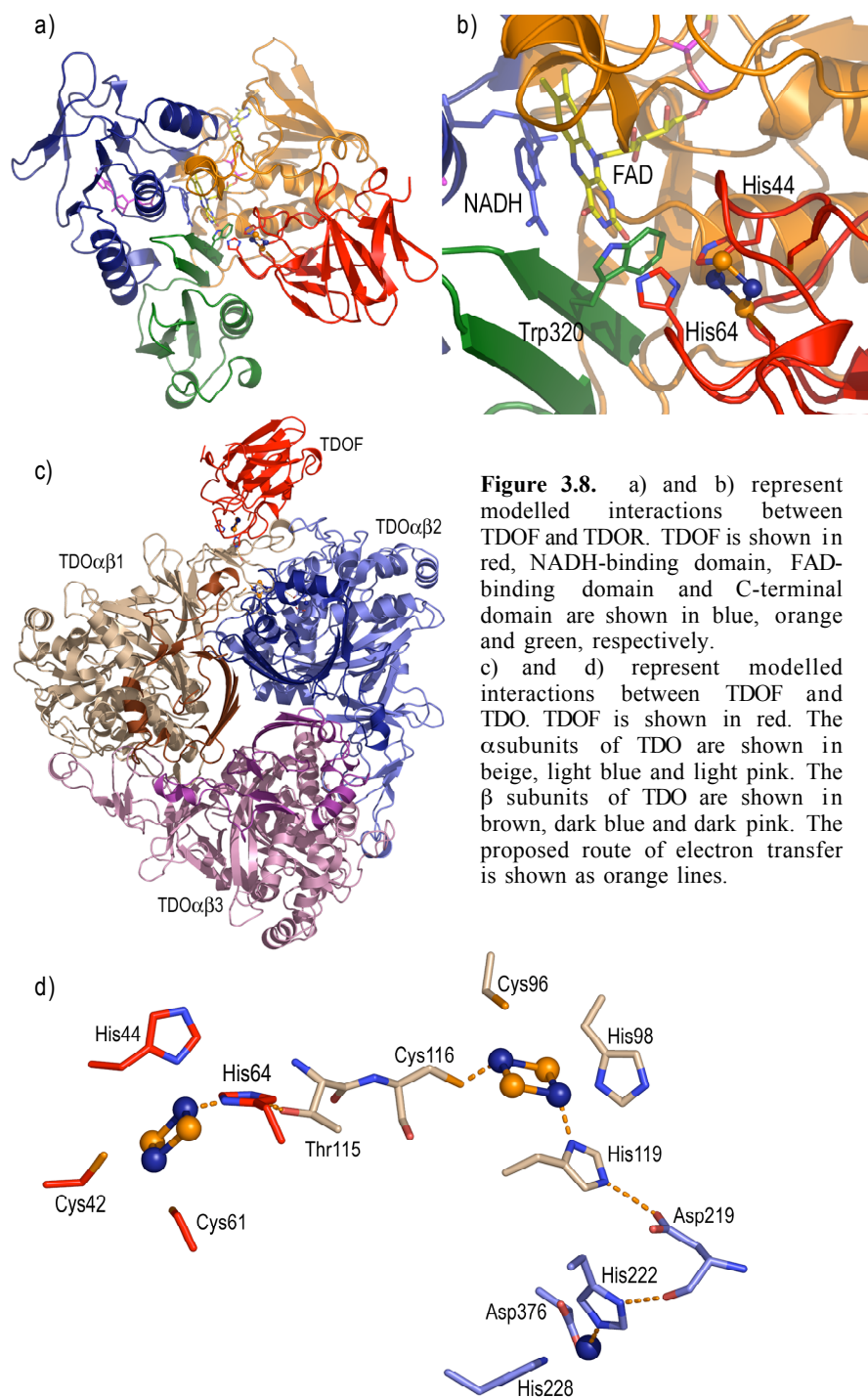
Initially two electrons are transferred from NADH in the hydride transfer to the FAD in the reductase. In front of the isoalloxazine ring of FAD in the TDOR structure there is a cavity that was found in BphA4 to be the NADH binding site (Senda *et al.*, 2000). Co-crystallization and soaking experiments of TDOR with NADH were unsuccessful. This is possibly due to an ammonium sulfate ion from the crystallization solution that could be located in the NADH binding pocket.

Hydrogen bonding from a water molecule and eight residues, all conserved between BphA4 and TDOR, hold the NADH in place in BphA4. Based on the structure of BphA4 it was possible to model the NADH molecule in the TDOR structure, where the nicotinamide ring is stacked approximately 3.5 Å from the isoalloxazine ring (Figure 3.8b).

TDOR comprise three shallow depressions that could be possible docking sites for TDOF. The most probable site for the one electron transfer from the FAD to the Rieske [2Fe-2S] cluster of TDOF is in the cleft between the C-terminal domain and the FAD-binding domain (Figure 3.8a). A His residue coordinating the Rieske center could be positioned about 6 Å from the N3 atom of the isoalloxazine ring. A conserved Trp that cover this edge of the flavin could mediate the electron transfer (Figure 3.8b).

When NDO, the first RDO structure was determined a putative ferredoxin binding site could be identified in a shallow depression close to the Rieske [2Fe-2S] cluster at the interface between two $\alpha\beta$ heterodimers (Kauppi *et al.*, 1998). An approach using the program FTDOCK and visual examination verified that the NDOF interacts with NDO at the proposed cavity (Karlsson, 2002). It was suggested that the electron transfer between the Rieske center of NDOF and NDO went through one of the histidines coordinating the Rieske center of NDOF via the main chain oxygen of a valine in NDO and its neighbouring Cys residue, which coordinate the Rieske center.

TDOF can be positioned similarly where the histidines coordinating the Rieske center are approximately 12 Å from the Rieske center of TDO (Figure 3.8c). The Val at the bottom of the NDO binding site is a Thr in TDO. One possible route of the electron transfer is via the side chain of the Thr and the cluster coordinating Cys of TDO (Figure 3.8d). The electron is then shuttled from the TDO Rieske center to the mononuclear iron in the neighbouring subunit via an absolutely conserved and crucial aspartate as previously described (Kauppi *et al.*, 1998; Parales *et al.*, 2000a).



3.5 The dioxygenation of nitroarene compounds (Paper V and VI)

Most nitroaromatic compounds are man-made and used extensively as industrial feedstocks for many manufacturing processes, including the production of pesticides, dyes and explosives. Because of improper storage, use and disposal nitroarene compounds have been released into the environment where they are considered serious environmental pollutants.

Many nitroaromatic compounds are known to be toxic. In addition nitrotoluenes are also known to be mutagenic and possibly carcinogenic (Couch *et al.*, 1981; Mirsalis and Butterworth, 1982; Tokiwa and Ohnishi, 1986; Bruning *et al.*, 2002).

Due to the more electronegative oxygen atoms of the nitro group, its nitrogen atom carries a partial positive charge and serves as an electrophile. This electron withdrawing property of the nitro group together with the stability of the benzene ring makes nitroarene compounds very difficult to degrade.

Industrially, wastewater containing nitroaromatic compounds is mostly degraded by chemical or sonochemical methods. However, interest for using biological methods are readily increasing.

In the naphthalene dioxygenase family of RDOs three different dioxygenases have been identified that degrade nitroaromatic compounds. These are nitrobenzene dioxygenase (NBDO) (Lessner *et al.*, 2002), 2-nitrotoluene dioxygenase (2NTDO) (Parales *et al.*, 1996) and 2,4-dinitrotoluene dioxygenase (DNTDO) (Suen *et al.*, 1996). Together with naphthalene dioxygenase (NDO) these four enzymes share approximately 80% sequence identity.

The nitroarene dioxygenases have different substrate specificities and can perform a monohydroxylation or a dihydroxylation reaction depending on the nitroarene-substrate and dioxygenase (Appendix A). In the dihydroxylation reaction the nitroarene dioxygenases add both atoms of dioxygen to a nitroarene nucleus, resulting in a nitro-dihydrodiol intermediate that undergoes spontaneous rearrangement to form a catechol with the accompanying release of nitrite (Figure 3.9).

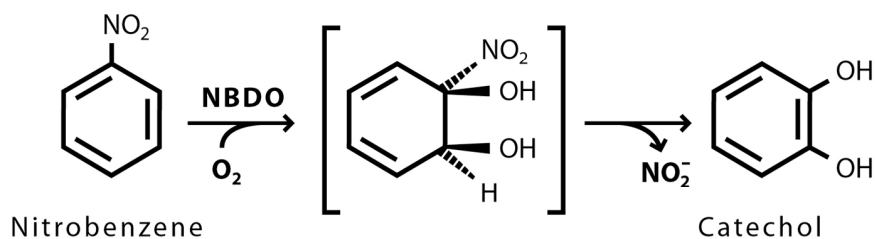


Figure 3.9. Dioxygenation of nitrobenzene catalyzed by NBDO.

3.5.1 Crystallization, data collection and structure solution of NBDO

NBDO was expressed and purified by our collaborators in Iowa City, IA, USA. Maja M. Ivkovic-Jensen found the initial crystallization conditions. The protein buffer was exchanged from BTGD (50 mM Bis-Tris, pH6.8, 5% glycerol, 1 mM sodium dithiothreitol) buffer to 50 mM MES, pH 6.8 prior to crystallization. NBDO (8-10 mg/ml) was crystallized by the vapor-diffusion technique. Initially hollow rods (Figure 3.10a) were obtained in 12% (w/v) polyethylene glycol 8000, 0.1M Tris buffer, pH 7.5 at 8°C. These crystals were not suitable for X-ray diffraction measurements and the crystallization conditions were further optimized. Addition of 5mM nickel sulfate made a radical change in the shape of the crystals to tulip shaped crystals (Figure 3.10b).

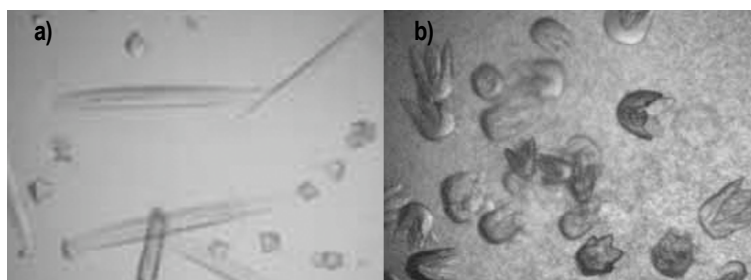


Figure 3.10. Crystals of NBDO. a) Hollow rods ($0.05 \times 0.05 \times 0.3 \text{ mm}^3$). b) Tulip shaped crystals ($0.1 \times 0.1 \times 0.2 \text{ mm}^3$).

X-ray diffraction data to 1.9 \AA were collected on beamline ID14-1 at the European Synchrotron Radiation Facility (ESRF), Grenoble, France on the base of a tulip shaped crystal. The crystals belong to the hexagonal spacegroup $P6_3$ where the asymmetric unit contain one $\alpha\beta$ heterodimer. The structure was solved by the molecular replacement program Molrep (Vagin and Teplyakov, 1997) using the fully reduced structure of NDO including all side chains as a search model. Data collection and refinement statistics are reported in Appendix B (NBDO).

An exogenous ligand was found outside the mononuclear iron atom in the active site. The ligand was interpreted as a Tris molecule from the crystallization solution (Figure 3.11). The iron atom has a distorted octahedral coordination where the NE atoms of His208 and His211, one carboxyl oxygen atom of Asp360, the nitrogen atom and the two oxygen atoms of the Tris molecule serve as ligands.

The crystallization conditions were again optimized where the Tris buffer was exchanged to various buffers. Crystals were obtained within 3-6 hours in 4-8% (w/v) polyethylene glycol 8000, 5mM NiCl_2 or 5mM NiSO_4 , 0.1 M MES, pH 6.0 or 0.1 M HEPES, pH 6.5 at 15-18 °C. Two crystal forms were obtained: hexagonal plates and tulip shaped crystals (Figure 3.12). Both crystal forms belonged to the space group $P6_3$. The tulip shaped crystals diffracted to 1.2 \AA whereas the hexagonal plates diffracted to 2 \AA .

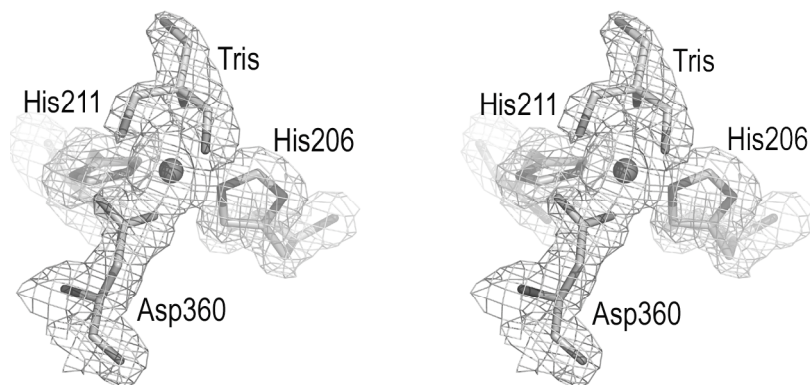


Figure 3.11. The mononuclear iron atom is coordinated by the side chains of His206, His211, Asp360 and by the nitrogen and two oxygen atoms of a Tris molecule from the crystallization solution. The $2F_{obs}-F_{calc}$ is contoured at 1σ .

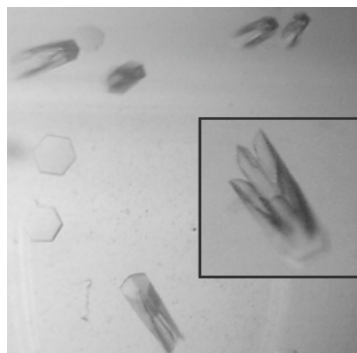


Figure 3.12. Crystals of NBDO. Hexagonal plates ($0.15 \times 0.15 \times 0.05 \text{ mm}^3$) and tulip shaped crystals ($0.15 \times 0.15 \times 0.3 \text{ mm}^3$).

3.5.2. Crystallization, data collection and structure solution of 2NTDO

2NTDO was expressed, purified and initially crystallized by Juan Parales. 2NTDO were crystallized by the vapor diffusion technique in 1.5-2.0 M Ammonium sulfate, 0.1M MES pH 6.8 at 8°C. Streak seeding were essential in order to obtain large enough crystals for data collection. X-ray diffraction data were collected at a CuK_α rotating-anode source at 100K. The crystals were pre-treated with a cryo solution consisting of the crystallization solution with an addition of 25% glycerol prior data collection. The crystals diffracted to 3.2 Å and belong to space group C2. One $\alpha_3\beta_3$ hetero-hexamer occupy the asymmetric unit corresponding to a solvent content of 82%. The structure was solved by molecular replacement using the NBDO $\alpha\beta$ heterodimer including all side chains as a search model. Data collection and refinement statistics are reported in Appendix B (2NTDO). Collection of X-ray diffraction data at a synchrotron source did not improve the resolution. The crystals suffered from radiation damage and a complete dataset could not be collected at a synchrotron source.

3.5.3 Overall structures of NBDO and 2NTDO.

NBDO and 2NTDO have a mushroom shaped $\alpha_3\beta_3$ hexameric structure as observed in NDO (Kauppi *et al.*, 1998) TDO and BphA1A2 (Furusawa *et al.*, 2004). The β subunits form the stem while the α subunits forms the cap of the mushroom. The α subunit of NBDO possesses two metal centers: a Rieske type [2Fe-2S] center and mononuclear iron at the active site.

The 2NTDO structure unfortunately lacked its mononuclear iron. Residues 205-235 including the two histidines coordinating the mononuclear iron could not be located in the electron density maps of 2NTDO. This is roughly the same region that becomes flexible in the structure of apo-TDO. No attempts have yet been made to reconstitute the mononuclear iron in 2NTDO.

3.5.4 Redox state of the Rieske center of NBDO

The redox state of the Rieske center was determined by measuring the UV-Vis spectra on crystals before and after data collection. The spectra were recorded on crystals under a cold stream of nitrogen at 100 K with a portable micro-spectrophotometer (Hadfield and Hajdu, 1993) mounted on an optical goniometer. The absorption spectra of the enzyme solution (Lessner, 2003) and that obtained from crystals correspond to the Rieske center in the oxidized state (Karlsson *et al.*, 2000) (Figure 3.13). Spectra recorded on crystals after data collection indicates the reduced state of the cluster, suggesting that X-ray radiation reduced the Rieske center.

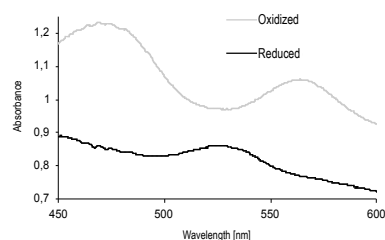


Figure 3.13. UV-Vis spectra of crystals before and after data collection. The spectra are recorded on two different crystals.

3.5.5 Comparison with other Rieske non-heme dioxygenases

Currently five RDO structures are known, where three belong to the Naphthalene family (NDO, NBDO and 2NTDO) and two to the Toluene/Biphenyl family (BphA1A2 and TDO). The structures are very similar suggesting that the core structures are highly conserved in this family of enzymes. The RMS deviations superpositioning the $\alpha\beta$ heterodimers range between 0.65 - 1.6 Å, where the RDO's within the naphthalene family can be superpositioned within 0.65 - 0.67 Å. Comparison within each family only reveals one significant structural difference located in the α subunit at the entrance of the active site in the loops between $\alpha 8$ - $\beta 13$ and $\beta 21$ - $\alpha 12$ (Appendix C). These loops are believed to act as lids covering the channel to the active site.

Comparisons of the structures of the two different RDO families show one major difference in the β subunit. The second half of the loop between $\beta 1$ - $\beta 2$ in NBDO, 2NTDO and NDO stacks against the Rieske domain of the α subunit. This part of the loop is more directed towards the β subunit with altered interactions with the Rieske domain in TDO and BphA1A2.

3.5.6 Soaking and co-crystallization of NBDO with aromatic substrates

Naphthalene dioxygenase in complex with different aromatic compounds were prepared by the soaking method (Carredano *et al.*, 2000; Karlsson *et al.*, 2003). The aromatic compounds were dissolved in ethanol to an extent where it could be mixed with the reservoir solution without precipitation. The crystals were soaked in this solution for 10-12 hours.

Extensive soaking trials of NBDO crystals with aromatic compounds by the same technique were all unsuccessful. None of the compounds tried; nitrobenzene, 3-nitrotoluene, naphthalene, naphthalene *cis*-dihydrodiol, indol, catechol and toluene bound at the active site. This was surprising since there are no crystal contacts at the entrance of the active site with neighbouring NBDO molecules. The loops covering the active site entrance are however positioned differently than in NDO, making the entrance narrower.

Co-crystallization with two different nitroaromatic compounds, nitrobenzene (NB) and 3-nitrotoluene (3NT) were shown to be victorious. The nitroaromatic compounds were mixed with ethanol to a final concentration of 1M. The ethanol solution was added to the reservoir to a final concentration of 50 mM. The nitroaromatic compounds were added in the same way to the cryoprotection solution.

3.5.7 Structures of NBDO in complex with nitrobenzene and 3-nitrotoluene

NBDO co-crystallized with NB and 3NT diffracted to 1.5 Å and 1.55 Å resolution respectively. NB and 3NT bind similarly in the flat and elongated substrate binding pocket of the α subunit. The substrate binding pocket is ranged by 17 residues where most residues, interacting with the aromatic substrates are hydrophobic. The methyl group of 3NT points towards the entrance of the active site (Figure 3.14). The oxygen atom closest to the mononuclear iron forms a hydrogen bond to the polar side chain of Asn258. The benzene ring of NB and 3NT are positioned about 5 Å away from the active site iron. Carbon atoms at position one and six undergo attack by dioxygen. These atoms are located closest to the mononuclear iron with the distances 4.7 Å and 4.4 Å respectively. The distances are similar to the dioxygen-attacked carbon atoms of naphthalene and the mononuclear iron in NDO (4.6 Å and 4.3 Å).

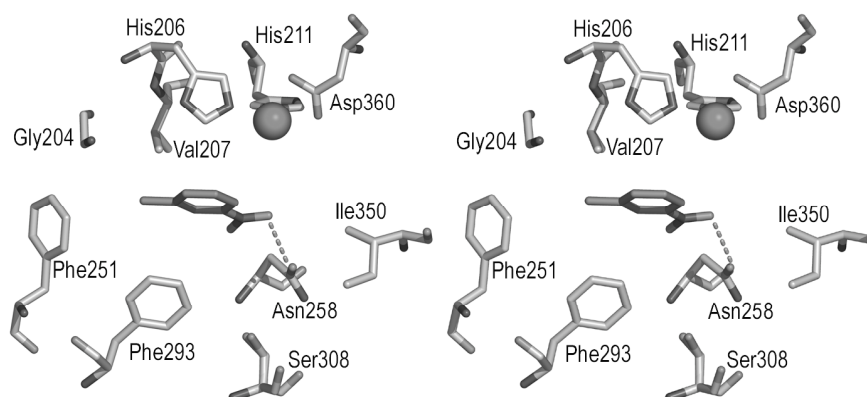


Figure 3.14. The active site of NBDO in complex with 3NT. Only residues coordinating the mononuclear iron and residues that are not conserved between NBDO, 2NTDO, NDO and DNTDO are represented.

3.5.8 Substrate specificity of NBDO, 2NTDO, NDO and DNTDO

Comparison of the active sites of NBDO and 2NTDO shows that only 3 residues differ in the substrate binding pocket between the enzymes. These are Gly204 (Ile in 2NTDO), Phe251 (Thr) and Phe293 (Ile) (Appendix C, Figure 3.15). Asn258 in 2NTDO probably hydrogen bonds to one of the oxygen atoms of the nitro group as seen in NBDO.

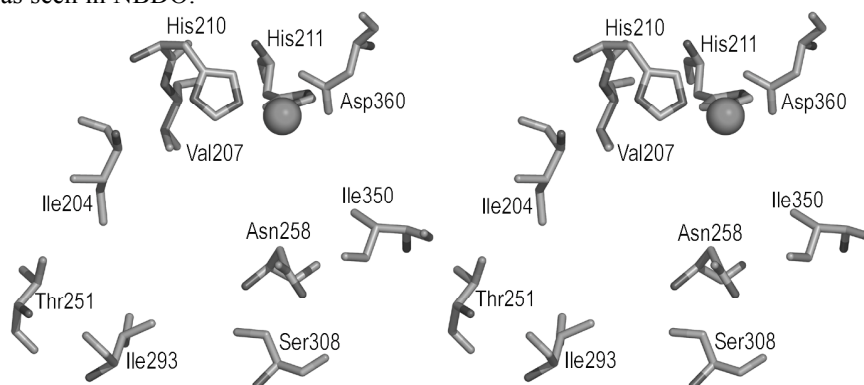


Figure 3.15. The active site of 2NTDO. The mononuclear iron, Val207, His210, His211, and Asp360 were not visible in the electron density maps and have been modelled in based on the structure of NBDO. Only residues coordinating the mononuclear iron and residues that are not conserved between NBDO, 2NTDO, NDO and DNIDO are represented.

NBDO and 2NTDO are the only known RDO's capable of oxidizing nitrobenzene (Appendix A) and this is probably due to the presence of Asn258. The Asn258Val mutants of NBDO and 2NTDO change the substrate specificity such that the nitrobenzyl alcohol is the major product instead of catechol (Kon-San Ju and Rebecca Parales, personnel communication).

2NTDO gives a higher ratio of the dihydroxylated product for 2NT than NBDO. Phe293 in NBDO has an Ile in the corresponding position in 2NTDO that should provide space for the methyl group of 2NT resulting in a higher percentage of dihydroxylated product formed.

NBDO, 2NTDO and NDO, for which three-dimensional structures are known, can all oxidize naphthalene to naphthalene *cis*-dihydrodiol (Appendix A). NDO is however unable to dihydroxylate nitroarene compounds and is only able to form nitrobenzyl alcohols from nitrotoluenes. For residues lining the active site, only five are different among the three enzymes (Appendix C, Figure 3.16). The corresponding residue for Asn258 in NBDO and 2NTDO is a Val in NDO. In NDO, the side chain of His295 is the only residue that can hydrogen bond to the nitrogroup of nitroaromatic compounds. Residue Phe352 in NDO, which is important for the regio- and enantioselectivity (Parales *et al.*, 2000b; Yu *et al.*, 2001), is larger than Ile350 in NBDO and 2NTDO and will hinder correct positioning of the nitroarene substrate for a dihydroxylation reaction to take place.

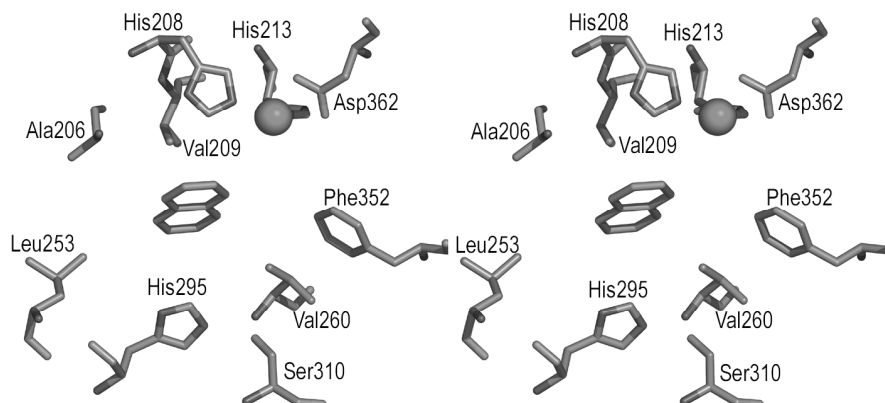


Figure 3.16. The active site of NDO in complex with naphthalene. Only residues coordinating the mononuclear iron and residues that are not conserved between NBDO, 2NTDO, NDO and DNTDO are represented.

DNTDO is like NDO unable to dihydroxylate NB and is only able to form nitrobenzyl alcohols from 2NT and 3NT. However, DNTDO can dihydroxylate 2,4-DNT to 4-methyl-5-nitrocatechol (Appendix C). To evaluate the active site structure of DNTDO a model has been made based on the structures of NBDO, 2NTDO and NDO (Figure 3.17). 2,4-DNT is a larger substrate than NB, 2NT, and 3NT. The substrate pocket in DNTDO must be able to accommodate the methyl group and provide hydrogen bonds to the two nitro groups. The side chains of residues Gln298 and Thr355 can hydrogen bond to one oxygen atom each of the two nitrogroups of 2,4-DNT.

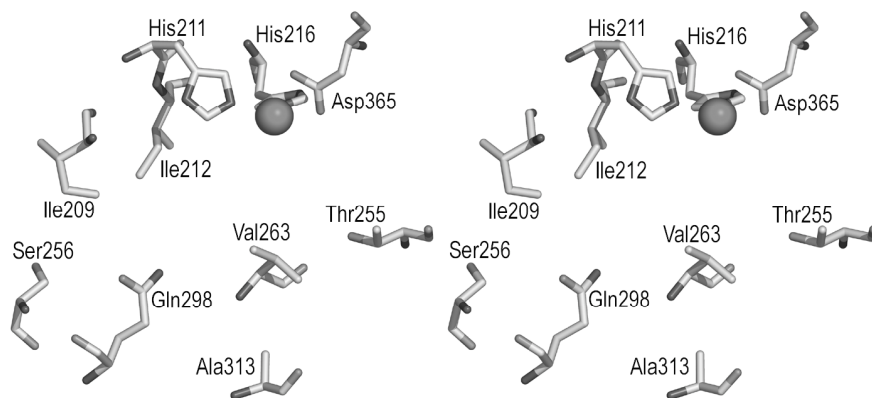


Figure 3.17. Model of the active site of DNTDO. Only residues coordinating the mononuclear iron and residues that are not conserved between NBDO, 2NTDO, NDO and DNTDO are represented.

NBDO, 2NTDO and NDO share a very high structural similarity. Only five residues in the active site differ between the enzymes, yet result in different substrate specificity and regioselectivity. The key residue for regioselectivity conferring *cis*-dihydroxylation of nitroarene compounds is presumably the presence of Asn258 that forms a hydrogen bond to the nitro-group of the substrates.

4. Future perspectives

The three-dimensional structure of the intermediate complex between FTR and Trx-*m* has provided insights into the catalytic mechanism of FTR. However, higher resolution of the complex structure is needed to resolve the detailed cluster geometry. In the third step of the FTR reaction a second electron is delivered by the next incoming ferredoxin. Ferredoxin can bind non-covalently to the FTR-Trx-*m* complex and crystallization trials of this triplex is currently being pursued.

The structures of the three-component TDO system have provided a good starting point for protein-protein docking studies to determine possible surface interactions during the electron transfer.

The suggested cleft of TDO that is proposed to bind the ferredoxin is solvent exposed in the crystals. In addition the solvent content is very high (> 80 %) which would make it possible to soak ferredoxin and get crystals of a TDO-TDOF complex.

The high resolution structures of NBDO in complexes with nitroarene substrates supply the first structural information on how nitroarene compounds are dioxygenated. The key residue for regioselectivity conferring *cis*-dihydroxylation is presumably the active site Asn258 that form a hydrogen bond to the nitro-group of the substrates.

Mutants with single and double amino acid substitutions in the active site of NBDO have been prepared in the lab of R.E. Parales. The characterization, accompanied with their structures in complex with nitroarene compounds will provide information about the role of each residue at the active site of NBDO.

References

- Adman, E. T., Sieker, L. C., Jensen, L. H., Bruschi, M. and Le Gall, J. (1977). A structural model of rubredoxin from *Desulfovibrio vulgaris* at 2 Å resolution. *J. Mol. Biol.* **112**, 113-20.
- Anastas, P. T. and Kirchhoff, M. M. (2002). Origins, current status, and future challenges of green chemistry. *Acc. Chem. Res.* **35**, 686-94.
- Antonkine, M. L., Jordan, P., Fromme, P., Krauss, N., Golbeck, J. H. and Stehlik, D. (2003). Assembly of protein subunits within the stromal ridge of photosystem I. Structural changes between unbound and sequentially PS I-bound polypeptides and correlated changes of the magnetic properties of the terminal iron sulfur clusters. *J. Mol. Biol.* **327**, 671-97.
- Arand, M., Hallberg, B. M., Zou, J., Bergfors, T., Oesch, F., van der Werf, M. J., de Bont, J. A., Jones, T. A. and Mowbray, S. L. (2003). Structure of *Rhodococcus erythropolis* limonene-1,2-epoxide hydrolase reveals a novel active site. *EMBO J.* **22**, 2583-92.
- Arner, E. S. and Holmgren, A. (2000). Physiological functions of thioredoxin and thioredoxin reductase. *Eur. J. Biochem.* **267**, 6102-9.
- Bassan, A., Blomberg, M. R. and Siegbahn, P. E. (2004). A theoretical study of the *cis*-dihydroxylation mechanism in naphthalene 1,2-dioxygenase. *J. Biol. Inorg. Chem.* **9**, 439-52.
- Batie, C. J., Ballou, D. P. and Corell, C. C. (1991). Phthalate dioxygenase reductase and related flavin-iron-sulfur containing electron transferases. Chemistry and biochemistry of flavoenzymes. F. Müller. Boca Raton, FL, CRC Press: 543-56.
- Beil, S., Mason, J. R., Timmis, K. N. and Pieper, D. H. (1998). Identification of chlorobenzene dioxygenase sequence elements involved in dechlorination of 1,2,4,5-tetrachlorobenzene. *J. Bacteriol.* **180**, 5520-8.
- Beinert, H., Holm, R.H., Munck, E. (1997). Iron-sulfur clusters: nature's modular, multipurpose structures. *Science* **277**, 653-9.
- Berkovitch, F., Nicolet, Y., Wan, J. T., Jarrett, J. T. and Drennan, C. L. (2004). Crystal structure of biotin synthase, an *S*-adenosylmethionine-dependent radical enzyme. *Science* **303**, 76-9.
- Berman, H. M., Westbrook, J., Feng, Z., Gilliland, G., Bhat, T. N., Weissig, H., Shindyalov, I. N. and Bourne, P. E. (2000). The Protein Data Bank. *Nucleic Acids Res.* **28**, 235-42.
- Boyd, D. R. and Sheldrake, G. N. (1998). The dioxygenase-catalysed formation of vicinal *cis*-diols. *Nat. Prod. Rep.* **15**, 309-24.
- Bruning, T., Thier, R. and Bolt, H. M. (2002). Nephrotoxicity and nephrocarcinogenicity of dinitrotoluene: new aspects to be considered. *Rev. Environ. Health* **17**, 163-72.
- Buchanan, B., Schürmann, P., Wolosiuk, R. and Jacquot, J. (2002). The ferredoxin/thioredoxin system: from discovery to molecular structures and beyond. *Photosynth. Res.* **73**, 215-22.
- Buchanan, B. B. (1980). Role in the light in the regulation of chloroplast enzymes. *Ann. Rev. Plant Phys.* **31**, 341-64.
- Buchanan, B. B. (1991). Regulation of CO₂ assimilation in oxygenic photosynthesis: the ferredoxin/thioredoxin system. Perspective on its discovery, present status, and future development. *Arch. Biochem. Biophys.* **288**, 1-9.
- Bullock, T. L., Clarkson, W. D., Kent, H. M. and Stewart, M. (1996). The 1.6 Å resolution crystal structure of nuclear transport factor 2 (NTF2). *J. Mol. Biol.* **260**, 422-31.
- Capitani, G., Markovic-Housley, Z., DelVal, G., Morris, M., Jansonius, J. N. and Schürmann, P. (2000). Crystal structures of two functionally different thioredoxins in spinach chloroplasts. *J. Mol. Biol.* **302**, 135-54.
- Carr, P. D., Verger, D., Ashton, A. R. and Ollis, D. L. (1999). Chloroplast NADP-malate dehydrogenase: structural basis of light-dependent regulation of activity by thiol oxidation and reduction. *Structure* **7**, 461-75.

- Carredano, E., Karlsson, A., Kauppi, B., Choudhury, D., Parales, R. E., Parales, J. V., Lee, K., Gibson, D. T., Eklund, H. and Ramaswamy, S. (2000). Substrate binding site of naphthalene 1,2-dioxygenase: functional implications of indole binding. *J. Mol. Biol.* **296**, 701-12.
- Carrell, C. J., Zhang, H., Cramer, W. A. and Smith, J. L. (1997). Biological identity and diversity in photosynthesis and respiration: structure of the lumen-side domain of the chloroplast Rieske protein. *Structure* **5**, 1613-25.
- Chiadmi, M., Navaza, A., Miginiac-Maslow, M., Jacquot, J. P. and Cherfils, J. (1999). Redox signalling in the chloroplast: structure of oxidized pea fructose-1,6-bisphosphate phosphatase. *EMBO J.* **18**, 6809-15.
- Chivers, P. T. and Raines, R. T. (1997). General acid/base catalysis in the active site of *Escherichia coli* thioredoxin. *Biochemistry* **36**, 15810-6.
- Colbert, C. L., Couture, M. M., Eltis, L. D. and Bolin, J. T. (2000). A cluster exposed: structure of the Rieske ferredoxin from biphenyl dioxygenase and the redox properties of Rieske Fe-S proteins. *Structure Fold. Des.* **8**, 1267-78.
- Correll, C. C., Batic, C. J., Ballou, D. P. and Ludwig, M. L. (1992). Phthalate dioxygenase reductase: a modular structure for electron transfer from pyridine nucleotides to [2Fe-2S]. *Science* **258**, 1604-10.
- Couch, D. B., Allen, P. F. and Abernethy, D. J. (1981). The mutagenicity of dinitrotoluenes in *Salmonella typhimurium*. *Mutat. Res.* **90**, 373-83.
- Dai, S., Schwendtmayer, C., Johansson, K., Ramaswamy, S., Schürmann, P. and Eklund, H. (2000a). How does light regulate chloroplast enzymes? Structure-function studies of the ferredoxin/thioredoxin system. *Q. Rev. Biophys.* **33**, 67-108.
- Dai, S., Schwendtmayer, C., Schürmann, P., Ramaswamy, S. and Eklund, H. (2000b). Redox signaling in chloroplasts: cleavage of disulfides by an iron-sulfur cluster. *Science* **287**, 655-8.
- Dyson, H. J., Jeng, M. F., Tennant, L. L., Slaby, I., Lindell, M., Cui, D. S., Kuprin, S. and Holmgren, A. (1997). Effects of buried charged groups on cysteine thiol ionization and reactivity in *Escherichia coli* thioredoxin: structural and functional characterization of mutants of Asp 26 and Lys 57. *Biochemistry* **36**, 2622-36.
- Ellis, P. J., Conrads, T., Hille, R. and Kuhn, P. (2001). Crystal structure of the 100 kDa arsenite oxidase from *Alcaligenes faecalis* in two crystal forms at 1.64 Å and 2.03 Å. *Structure (Camb.)* **9**, 125-32.
- Fairlamb, A. H. and Cerami, A. (1992). Metabolism and functions of trypanothione in the Kinetoplastida. *Annu. Rev. Microbiol.* **46**, 695-729.
- Friemann, R., Schmidt, H., Ramaswamy, S., Forstner, M., Krauth-Siegel, R. L. and Eklund, H. (2003). Structure of thioredoxin from *Trypanosoma brucei brucei*. *FEBS Lett.* **554**, 301-5.
- Furusawa, Y., Nagarajan, V., Tanokura, M., Masai, E., Fukuda, M. and Senda, T. (2004). Crystal structure of the terminal oxygenase component of biphenyl dioxygenase derived from *Rhodococcus* sp. strain RHA1. *J. Mol. Biol.* **342**, 1041-52.
- Gajhede, M., Osmark, P., Poulsen, F. M., Ipsen, H., Larsen, J.N., Joost van Neerven, R. J., Schou, C., Lowenstein, H. and Spangfort, M. D. (1996). X-ray and NMR structure of Bet v 1, the origin of birch pollen allergy. *Nat. Struct. Biol.* **3**, 1040-5.
- Gassner, G. T., Ludwig, M. L., Gatti, D. L., Correl, C. C. and Ballou, D. P. (1995). Structure and mechanism of the iron-sulfur flavoprotein phthalate dioxygenase reductase. *FASEB J.* **9**, 1411-8.
- Gibson, D. T., Hensley, M., Yoshioka, H. and Mabry, T. J. (1970). Formation of (+)-cis-2,3-dihydroxy-1-methylcyclohexa-4,6-diene from toluene by *Pseudomonas putida*. *Biochemistry* **9**, 1626-30.
- Gibson, D. T., Koch, J. R. and Kallio, R. E. (1968). Oxidative degradation of aromatic hydrocarbons by microorganisms. I. Enzymatic formation of catechol from benzene. *Biochemistry* **7**, 2653-62.
- Gibson, D. T. and Parales, R. E. (2000). Aromatic hydrocarbon dioxygenases in environmental biotechnology. *Curr. Opin. Biotechnol.* **11**, 236-43.
- Greenberg, M. M. (1997). The central nervous system and exposure to toluene: a risk characterization. *Environ. Res.* **72**, 1-7.

- Gromer, S., Urig, S. and Becker, K. (2004). The thioredoxin system-From science to clinic. *Med. Res. Rev.* **24**, 40-89.
- Hadfield, A. and Hajdu, J. (1993). A Fast and Portable Microspectrophotometer for Protein Crystallography. *J. Appl. Crystallogr.* **26**, 839-42.
- Hall, D. O., Cammack, R. and Rao, K. K. (1971). Role for ferredoxins in the origin of life and biological evolution. *Nature* **233**, 136-8.
- Hoelz, A., Nairn, A. C. and Kuriyan, J. (2003). Crystal structure of a tetradecameric assembly of the association domain of Ca²⁺/calmodulin-dependent kinase II. *Mol. Cell* **11**, 1241-51.
- Holmgren, A. (1985). Thioredoxin. *Annu. Rev. Biochem.* **54**, 237-71.
- Holmgren, A. (1995). Thioredoxin structure and mechanism: conformational changes on oxidation of the active-site sulfhydryls to a disulfide. *Structure* **3**, 239-43.
- Hudlicky, T., Gonzalez, D. and Gibson, D. T. (1999). Enzymatic dihydroxylation of aromatics in enantioselectivity synthesis: Expanding asymmetric methodology. *Aldrichimica Acta* **32**, 35-62.
- Hudlicky, T. and Reed, J. W. (1995). An evolutionary perspective of microbial oxidations of aromatic compounds in enantioselective synthesis: history, current status, and perspectives. *Advances in asymmetric synthesis*. A. Hassner. Greenwich, CT., JAI Press Inc. **1**: 271-312.
- Hunsicker-Wang, L. M., Heine, A., Chen, Y., Luna, E. P., Todaro, T., Zhang, Y. M., Williams, P. A., McRee, D. E., Hirst, J., Stout, C. D. and Fee, J. A. (2003). High-resolution structure of the soluble, respiratory-type Rieske protein from *Thermus thermophilus*: analysis and comparison. *Biochemistry* **42**, 7303-17.
- Hunt, J. F., van der Vies, S.M., Henry, L., Deisenhofer, J. (1997). Structural adaptations in the specialized bacteriophage T4 co-chaperonin Gp31 expand the size of the Anfinsen cage. *Cell* **90**, 361-71.
- Iwata, S., Lee, J. W., Okada, K., Lee, J. K., Iwata, M., Rasmussen, B., Link, T. A., Ramaswamy, S. and Jap, B. K. (1998). Complete structure of the 11-subunit bovine mitochondrial cytochrome *bc*₁ complex. *Science* **281**, 64-71.
- Iwata, S., Saynovits, M., Link, T. A. and Michel, H. (1996). Structure of a water soluble fragment of the 'Rieske' iron-sulfur protein of the bovine heart mitochondrial cytochrome *bc*₁ complex determined by MAD phasing at 1.5 Å resolution. *Structure* **4**, 567-79.
- Iyer, L. M., Koonin, E. V. and Aravind, L. (2001). Adaptations of the helix-grip fold for ligand binding and catalysis in the START domain superfamily. *Proteins* **43**, 134-44.
- Jacquot, J.-P., Lancelin, J.-M. and Meyer, Y. (1997). Thioredoxins: structure and function in plant cells. *New Phytol.* **136**, 543-70.
- Jameson, G. N., Walters, E. M., Manieri, W., Schürmann, P., Johnson, M. K. and Huynh, B. H. (2003). Spectroscopic evidence for site specific chemistry at a unique iron site of the [4Fe-4S] cluster in ferredoxin:thioredoxin reductase. *J. Am. Chem. Soc.* **125**, 1146-7.
- Jiang, H., Parales, R. E. and Gibson, D. T. (1999). The α subunit of toluene dioxygenase from *Pseudomonas putida* F1 can accept electrons from reduced Ferredoxin_{TOL} but is catalytically inactive in the absence of the β subunit. *Appl. Environ. Microbiol.* **65**, 315-8.
- Johansson, K., Ramaswamy, S., Saarinen, M., Lemaire-Chamley, M., Issakidis-Bourguet, E., Miginiac-Maslow, M. and Eklund, H. (1999). Structural basis for light activation of a chloroplast enzyme: the structure of sorghum NADP-malate dehydrogenase in its oxidized form. *Biochemistry* **38**, 4319-26.
- Jordan, P., Fromme, P., Witt, H. T., Klukas, O., Saenger, W. and Krauss, N. (2001). Three-dimensional structure of cyanobacterial photosystem I at 2.5 Å resolution. *Nature* **411**, 909-17.
- Karlsson, A. (2002). Structural and mechanistic studies of Rieske dioxygenases. Department of Molecular Biology. Uppsala, The Swedish University of Agricultural Sciences.

- Karlsson, A., Beharry, Z. M., Matthew Eby, D., Coulter, E. D., Neidle, E. L., Kurtz, D. M., Jr., Eklund, H. and Ramaswamy, S. (2002). X-ray crystal structure of benzoate 1,2-dioxygenase reductase from *Acinetobacter* sp. strain ADP1. *J. Mol. Biol.* **318**, 261-72.
- Karlsson, A., Parales, J. V., Parales, R. E., Gibson, D. T., Eklund, H. and Ramaswamy, S. (2000). The reduction of the Rieske iron-sulfur cluster in naphthalene dioxygenase by X-rays. *J. Inorg. Biochem.* **78**, 83-7.
- Karlsson, A., Parales, J. V., Parales, R. E., Gibson, D. T., Eklund, H. and Ramaswamy, S. (2003). Crystal structure of naphthalene dioxygenase: side-on binding of dioxygen to iron. *Science* **299**, 1039-42.
- Karplus, P. A. and Schulz, G. E. (1989). Substrate binding and catalysis by glutathione reductase as derived from refined enzyme: substrate crystal structures at 2 Å resolution. *J. Mol. Biol.* **210**, 163-80.
- Kauppi, B., Lee, K., Carredano, E., Parales, R. E., Gibson, D. T., Eklund, H. and Ramaswamy, S. (1998). Structure of an aromatic-ring-hydroxylating dioxygenase-naphthalene 1,2-dioxygenase. *Structure* **6**, 571-86.
- Kerfeld, C. A., Sawaya, M. R., Brahmamdam, V., Cascio, D., Ho, K. K., Trevithick-Sutton, C. C., Krogmann, D. W. and Yeates, T. O. (2003). The crystal structure of a cyanobacterial water-soluble carotenoid binding protein. *Structure (Camb.)* **11**, 55-65.
- Kim, S. W., Cha, S. S., Cho, H. S., Kim, J. S., Ha, N. C., Cho, M. J., Joo, S., Kim, K. K., Choi, K. Y. and Oh, B. H. (1997). High-resolution crystal structures of Δ^3 -3-ketosteroid isomerase with and without a reaction intermediate analogue. *Biochemistry* **36**, 14030-6.
- Kobal, V. M., Gibson, D. T., Davis, R. E. and Garza, A. (1973). X-ray determination of the absolute stereochemistry of the initial oxidation product formed from toluene by *Pseudomonas putida* 39-D. *J. Am. Chem. Soc.* **95**, 4420-1.
- Krauth-Siegel, R. L. and Coombs, G. H. (1999). Enzymes of parasite thiol metabolism as drug targets. *Parasitol. Today* **15**, 404-9.
- Lau, P. C. K. and De Lorenzo, V. (1999). Genetic engineering: The frontier of bioremediation. *Environ. Sci. Technol.* **33**, 124A-8A.
- LeMaster, D. M., Springer, P. A. and Unkefer, C. J. (1997). The role of the buried aspartate of *Escherichia coli* thioredoxin in the activation of the mixed disulfide intermediate. *J. Biol. Chem.* **272**, 29998-30001.
- Lessner, D. J. (2003). Molecular characterization of Rieske non-heme iron dioxygenases involved in nitroarene and naphthalene degradation. Department of Microbiology. Iowa City, The University of Iowa.
- Lessner, D. J., Johnson, G. R., Parales, R. E., Spain, J. C. and Gibson, D. T. (2002). Molecular characterization and substrate specificity of nitrobenzene dioxygenase from *Comamonas* sp. strain JS765. *Appl. Environ. Microbiol.* **68**, 634-41.
- Lim, D. and Strynadka, N. C. (2002). Structural basis for the β lactam resistance of PBP2a from methicillin-resistant *Staphylococcus aureus*. *Nat. Struct. Biol.* **9**, 870-6.
- Lloyd, S. J., Lauble, H., Prasad, G. S. and Stout, C. D. (1999). The mechanism of aconitase: 1.8 Å resolution crystal structure of the S642A:citrate complex. *Protein Sci.* **8**, 2655-62.
- Lundqvist, T., Rice, J., Hodge, N., Basarab, G., Pierce, J. and Lindqvist, Y. (1994). Crystal structure of scytalone dehydratase - a disease determinant of the rice pathogen, *Magnaporthe grisea*. *Structure* **2**, 937-44.
- Mate, M. J., Ortiz-Lombardia, M., Boitel, B., Haouz, A., Tello, D., Susin, S. A., Penninger, J., Kroemer, G. and Alzari, P. M. (2002). The crystal structure of the mouse apoptosis-inducing factor AIF. *Nat. Struct. Biol.* **9**, 442-6.
- Menchise, V., Corbier, C., Didierjean, C., Saviano, M., Benedetti, E., Jacquot, J. P. and Aubry, A. (2001). Crystal structure of the wild-type and D30A mutant thioredoxin *h* of *Chlamydomonas reinhardtii* and implications for the catalytic mechanism. *Biochem J* **359**, 65-75.
- Meyer, J. (2001). Ferredoxins of the third kind. *FEBS Lett.* **509**, 1-5.

- Mirsalis, J. C. and Butterworth, B. E. (1982). Induction of unscheduled DNA synthesis in rat hepatocytes following in vivo treatment with dinitrotoluene. *Carcinogenesis* **3**, 241-5.
- Myler, P. J., Audleman, L., deVos, T., Hixson, G., Kiser, P., Lemley, C., Magness, C., Rickel, E., Sisk, E., Sunkin, S., Swartzell, S., Westlake, T., Bastien, P., Fu, G., Ivens, A. and Stuart, K. (1999). *Leishmania major* Friedlin chromosome 1 has an unusual distribution of protein-coding genes. *Proc. Natl. Acad. Sci. U. S. A.* **96**, 2902-6.
- Nikkola, M. (1991). Structural and functional studies on glutaredoxin and thioredoxin. Uppsala, Sweden, Swedish University of Agricultural Sciences.
- Parales, J. V., Kumar, A., Parales, R. E. and Gibson, D. T. (1996). Cloning and sequencing of the genes encoding 2-nitrotoluene dioxygenase from *Pseudomonas* sp. JS42. *Gene* **181**, 57-61.
- Parales, J. V., Parales, R. E., Resnick, S. M. and Gibson, D. T. (1998a). Enzyme specificity of 2-nitrotoluene 2,3-dioxygenase from *Pseudomonas* sp. strain JS42 is determined by the C-terminal region of the alpha subunit of the oxygenase component. *J. Bacteriol.* **180**, 1194-9.
- Parales, R. E., Emig, M. D., Lynch, N. A. and Gibson, D. T. (1998b). Substrate specificities of hybrid naphthalene and 2,4-dinitrotoluene dioxygenase enzyme systems. *J. Bacteriol.* **180**, 2337-44.
- Parales, R. E., Lee, K., Resnick, S. M., Jiang, H., Lessner, D. J. and Gibson, D. T. (2000a). Substrate specificity of naphthalene dioxygenase: effect of specific amino acids at the active site of the enzyme. *J. Bacteriol.* **182**, 1641-9.
- Parales, R. E., Resnick, S. M., Yu, C. L., Boyd, D. R., Sharma, N. D. and Gibson, D. T. (2000b). Regioselectivity and enantioselectivity of naphthalene dioxygenase during arene *cis*-dihydroxylation: control by phenylalanine 352 in the α subunit. *J. Bacteriol.* **182**, 5495-504.
- Powis, G. and Montfort, W. R. (2001). Properties and biological activities of thioredoxins. *Annu. Rev. Biophys. Biomol. Struct.* **30**, 421-55.
- Reckenfelderbäumer, N., Lüdemann, H., Schmidt, H., Steverding, D. and Krauth-Siegel, R. L. (2000). Identification and functional characterization of thioredoxin from *Trypanosoma brucei brucei*. *J. Biol. Chem.* **275**, 7547-52.
- Resnick, S. M., Lee, K. and Gibson, D. T. (1996). Diverse reactions catalyzed by naphthalene dioxygenase from *Pseudomonas* sp strain ncib 9816. *J. Ind. Microbiol. Biotechnol.* **17**, 438-57.
- Robbins, A. H. and Stout, C. D. (1989). Structure of activated aconitase: formation of the [4Fe-4S] cluster in the crystal. *Proc. Natl. Acad. Sci. U S A* **86**, 3639-43.
- Romanowski, M. J., Soccio, R. E., Breslow, J. L. and Burley, S. K. (2002). Crystal structure of the *Mus musculus* cholesterol-regulated START protein 4 (StarD4) containing a StAR-related lipid transfer domain. *Proc. Natl. Acad. Sci. U S A* **99**, 6949-54.
- Scheibe, R. (1994). Photoregulation of chloroplast enzymes. *Naturwissenschaften* **81**, 443-8.
- Schulz, G. E., Schirmer, R. H., Sachsenheimer, W. and Pai, E. F. (1978). The structure of the flavoenzyme glutathione reductase. *Nature* **273**, 120-4.
- Schürmann, P. (2003). Redox Signaling in the Chloroplast - the Ferredoxin/Thioredoxin System. *Antioxid. Redox Signal.* **5**, 69-78.
- Schürmann, P. and Buchanan, B. B. (2001). The structure and function of the ferredoxin/thioredoxin system. in: Regulatory Aspects of Photosynthesis. Advances in Photosynthesis. B. Andersson and E. M. Aro. Dordrecht, The Netherlands, Kluwer Academic Publishers,.
- Senda, T., Yamada, T., Sakurai, N., Kubota, M., Nishizaki, T., Masai, E., Fukuda, M. and Mitsuidagger, Y. (2000). Crystal structure of NADH-dependent ferredoxin reductase component in biphenyl dioxygenase. *J. Mol. Biol.* **304**, 397-410.
- Sheldrake, G. N. (1992). Biologically derived arene *cis*-dihydrodiols as synthetic building blocks. Chirality in industry: the commercial manufacture and application of optically active compounds. G. N. S. A. N. C. a. J. Crosby. Chichester, UK, John Wiley & Sons Ltd.: 127-66.

- Staples, C. R., Ameyibor, E., Fu, W., Gardet-Salvi, L., Stritt-Etter, A. L., Schürmann, P., Knaff, D. B. and Johnson, M. K. (1996). The function and properties of the iron-sulfur center in spinach ferredoxin: thioredoxin reductase: a new biological role for iron-sulfur clusters. *Biochemistry* **35**, 11425-34.
- Suen, W. C., Haigler, B. E. and Spain, J. C. (1996). 2,4-Dinitrotoluene dioxygenase from *Burkholderia* sp. strain DNT: similarity to naphthalene dioxygenase. *J. Bacteriol.* **178**, 4926-34.
- Tan, H. M. and Cheong, C. M. (1994). Substitution of the ISP α subunit of biphenyl dioxygenase from *Pseudomonas* results in a modification of the enzyme activity. *Biochem. Biophys. Res. Commun.* **204**, 912-7.
- Tokiwa, H. and Ohnishi, Y. (1986). Mutagenicity and carcinogenicity of nitroarenes and their sources in the environment. *Crit. Rev. Toxicol.* **17**, 23-60.
- Tsujishita, Y. and Hurley, J. H. (2000). Structure and lipid transport mechanism of a StAR-related domain. *Nat. Struct. Biol.* **7**, 408-14.
- Vagin, A. and Teplyakov, A. (1997). MOLREP: an automated program for molecular replacement. *J. Appl. Crystallogr.* **30**, 1022-5.
- Villeret, V., Huang, S., Zhang, Y., Xue, Y., Lipscomb, W.N. (1995). Crystal structure of spinach chloroplast fructose-1,6-bisphosphatase at 2.8 Å resolution. *Biochemistry* **34**, 4299-306.
- Volbeda, A., Charon, M. H., Piras, C., Hatchikian, E. C., Frey, M. and Fontecilla-Camps, J. C. (1995). Crystal structure of the nickel-iron hydrogenase from *Desulfovibrio gigas*. *Nature* **373**, 580-7.
- Williams, C. H., Jr. (1992). Lipoamide dehydrogenase, glutathione reductase, thioredoxin reductase, and mercury ion reductase - a family of flavoenzyme transhydrogenases. Chemistry and Biochemistry of Flavoenzymes. F. Müller. Boca Raton, FL., CRC Press. **III**: 121-211.
- Wolfe, M. D., Parales, J. V., Gibson, D. T. and Lipscomb, J. D. (2001). Single turnover chemistry and regulation of O₂ activation by the oxygenase component of naphthalene 1,2-dioxygenase. *J. Biol. Chem.* **276**, 1945-53.
- Ye, H., Cande, C., Stephanou, N. C., Jiang, S., Gurbuxani, S., Larochette, N., Daugas, E., Garrido, C., Kroemer, G. and Wu, H. (2002). DNA binding is required for the apoptogenic action of apoptosis inducing factor. *Nat. Struct. Biol.* **9**, 680-4.
- Yoder, M. D., Thomas, L. M., Tremblay, J. M., Oliver, R. L., Yarbrough, L. R. and Helmkamp, G. M., Jr. (2001). Structure of a multifunctional protein. Mammalian phosphatidylinositol transfer protein complexed with phosphatidylcholine. *J. Biol. Chem.* **276**, 9246-52.
- Yu, C. L., Parales, R. E. and Gibson, D. T. (2001). Multiple mutations at the active site of naphthalene dioxygenase affect regioselectivity and enantioselectivity. *J. Ind. Microbiol. Biotechnol.* **27**, 94-103.

• Tack • धन्यवाद • Thank you • 감사합니다 •
• Vielen Dank • 谢谢 • Merci • Спасибо •

My dear supervisors, you are the true definition of Jin and Jang! It has been a great pleasure working with you. **Hasse**, thank you for all the support and for always being so optimistic. Thank you **Rams** for your endless energy, for always answering all my questions and finding new projects when old ones won't work.

Thank you all great collaborators! **David** and **Rebecca**, for your interest and support. **Chi-Li** for happily putting up hundreds of crystallization trials on NDOR! **Maja** for believing in tulip shaped crystals. **Kyoung** and **Juan** for having magical crystallization fingers. Thank you **Bosse**, **Myroslawa**, **Peter** and **Shaodong**.

Malin, Thank you for all these great years and for making our office such a happy place! Good luck with Herman/Hermione!

Thank you **Wendie**, **Dr. Allen** and **Modestos** for all the fun! **Modestos** for all the crazy discussions at the JAVA house. **Tom** for your great sense of humour and for your wonderful personality. **Wendie** for your friendship, fun blues nights and for keeping order of the boys in the lab (including Rams).

Andreas, my man. Thank you for all your support and discussions. **Urszula**, thanks for being such a great person. Thank you **Andrea** for fantastic skiing trips to Romme. **Fredrik** for your passion for “slem” and your moves on the dance floor. Monsieur **Welin** for teaching me everything about Dafgård. **Vladimir** for always being so happy and helpful and of course for your “short questions”. Good luck with your new baby **Nisse** and thanks for always knowing what version of CCP4 to download. Also thanks to **Kenth** and **Deva** for all your help when I started my studies. Good luck **Pontus**, **Louise** and **Lotta**.

Nathan, you are the most enthusiastic person I ever met! Thank you for great music and good luck with your Ph.D. Thank you **Lokesh** for teaching me how to cryo-cool crystals. Best of luck, **Dan**, **Jon**, **Emmanuel** (my “blood” brother!), **Adam** and **Eric**. Thank you **Bryce** for good advice and for always being a true gentleman. Thank you **Tam**, **Greta**, **Travis**, **Wendy**, **Lena**, and **Dipi**! **Bill**, **Lori**, **Brenda** and **Mary**, many thanks for always being so helpful.

Thank you **alla@xray** for making this place such a great place to work.

Talal for being so fabulous, **Karin** for all your help and support, **Janos** for being so inspiring, **Inger** for the best synchrotron bag. **Alwyn** for asking questions at Friday seminars. Thank you **Lars** for teaching me crystallography. Thank you **Anke** for teaching me crystallography for the second time and sharing our first experience as “bag ladies”! Thank you **Al, Jenny, Daniel** and **Annette** and all the other beer kings and queens. **Linda, Emma, Inez, Eva-Lena and Sara**, thanks for being great gals! It takes a ponytail to manage the Mol. Biol. Department. Thank you **Ulla** and **Stefan** for running it. Thank you **Saeid** for Frank Sinatra songs and being the master of British roundabouts.

Erling, Christer, Remco and **David**, thank you for all the help! Thank you **Margareta** for planning the teaching and for keeping order in the lab. Good luck **Nic** with your baby. Thank you **Tex** for your great book and all crystallization tips. Thank you **Seved, Nina, Fredrik, Jens, Sinisa, Stefan, Johan, Midi, Maxi** and **Efti** for great company during coffee breaks. **Mark**, thanks for the ice skating tours. Thank you **Gerard** and **Henrik** for the greatest conferences, **Patrik** and **Fariborz** for interesting discussions, **Wimal** for being so nice.

Thank you **Wojtec, Agata, Tom, Hugo, Albert, Ola, Gisela, Alexandra, Magnus, Carl, Gösta, Johan, Jimmy, Alina, Lena, Gunnar, Susanna, Marian, Tove, Karl, Jerry, Anton, Ulrica, Totte, Sherry, Elin, Gunilla, Diane, Martin, Llano, Lollo,.....**

Thank you **Vladimir** and **Olga** for all the chocolate and fruits during synchrotron trips. It is so great that you can continue with this tradition!

Tack **Hans** och **Mälle** för de bästa brorsbarnen.

Mamma och **Pappa**, tack för att ni alltid har stöttat mig i allt!

Sasha, thanks for your love and for being such a wonderful person.